AD-A150 667 TRANSONIC MERGING SEPARATED FLOWS(U) MISSISSIPPI STATE 1/2
UNIV MISSISSIPPI STATE DEPT OF AEROPHYSICS AND
AEROSPACE ENGINEERING K KOENIG JUL 84 AFOSR-TR-85-0096
UNCLASSIFIED AFOSR-83-0179 F/G 20/4 NL

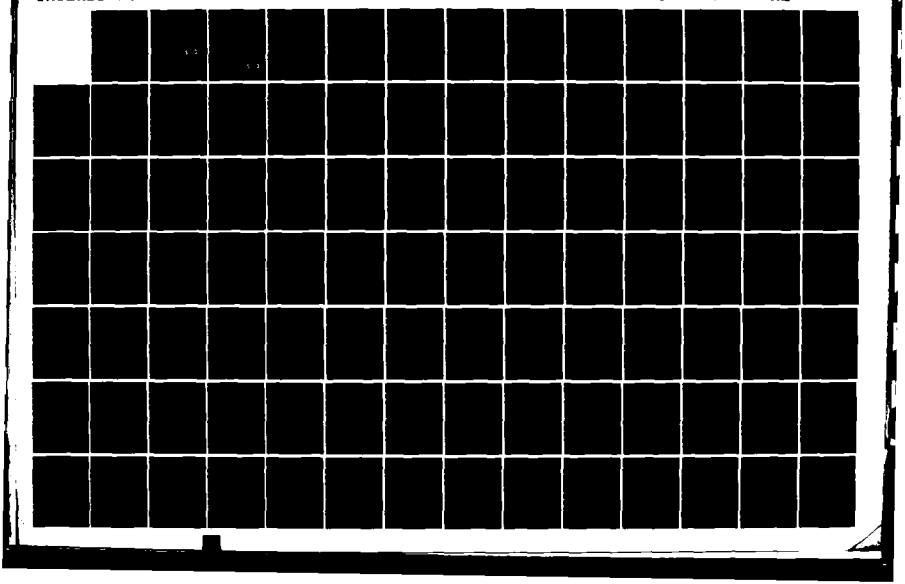

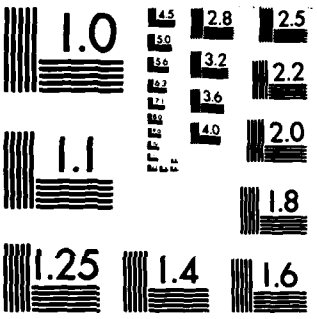

(2)

AFOSR-TR- 85-0096

TRANSONIC MERGING SEPARATED FLOWS

Keith Koenig

Department of Aerospace Engineering
Mississippi State University
July 1984

Sponsored by the Air Force Office of Scientific Research
under AFOSR grant 83-0179

Approved for Public Release; Distribution Unlimited

TRANSONIC MERGING SEPARATED FLOWS

Keith Koenig

Department of Aerospace Engineering
Mississippi State University
July 1984

Sponsored by the Air Force Office of Scientific Research
under AFOSR grant 83-0179

"Qualified requestors may obtain additional copies from the Defense Technical Information Services."

UNCLASSIFIED

SECURITY CLASSIFICATION OF THIS PAGE (When Data Entered)

REPORT DOCUMENTATION PAGE	READ INSTRUCTIONS BEFORE COMPLETING FORM
1. REPORT NUMBER: AFOSR-TR- 85-0096	2. GOVT ACCESSION NO.: AD-A150 667
	3. RECIPIENT'S CATALOG NUMBER:
4. TITLE (and Subtitle): TRANSONIC MERGING SEPARATED FLOWS	5. TYPE OF REPORT & PERIOD COVERED: FINAL 1 MAY 83 TO 30 APR 84
	6. PERFORMING ORG. REPORT NUMBER:
7. AUTHOR(s): KEITH KOENIG	8. CONTRACT OR GRANT NUMBER(s): AFOSR 83-0179
9. PERFORMING ORGANIZATION NAME AND ADDRESS: MISSISSIPPI STATE UNIVERSITY, DEPARTMENT OF AEROSPACE ENGINEERING, MISSISSIPPI STATE, MS 39762	10. PROGRAM ELEMENT, PROJECT, TASK AREA & WORK UNIT NUMBERS: 61102F 2307 D9
11. CONTROLLING OFFICE NAME AND ADDRESS: Dr. James Wilson, AFOSR/NA, Bolling AFB, DC 20332 202/767-4935	12. REPORT DATE: 1984, July
	13. NUMBER OF PAGES: 96
14. MONITORING AGENCY NAME & ADDRESS(if different from Controlling Office)	15. SECURITY CLASS. (of this report): Unclassified
	15a. DECLASSIFICATION/DOWNGRADING SCHEDULE:

16. DISTRIBUTION STATEMENT (of this Report)

Approved for Public Release;
Distribution Unlimited.

17. DISTRIBUTION STATEMENT (of the abstract entered in Block 20, if different from Report)

18. SUPPLEMENTARY NOTES

19. KEY WORDS (Continue on reverse side if necessary and identify by block number)

20. ABSTRACT (Continue on reverse side if necessary and identify by block number)

An arrangement of a plane-nosed circular cylinder with a smaller diameter plane-nosed cylindrical probe coaxially extending ahead in a transonic axial flow has been considered. This configuration is a prototype for a low drag forebody replacing more conventional streamlined nose fairings.

An attempt is made to construct a description of the flow field based on data for related and component flows. The flow is modelled as the merging of several component, separated flows. Component flows are axisymmetric plane-nosed cylinders and axisymmetric forward-facing steps. Related flows include

DD FORM 1 JAN 73 1473 EDITION OF 1 NOV 65 IS OBSOLETE
S/N 0102-LF-014-6601

UNCLASSIFIED

SECURITY CLASSIFICATION OF THIS PAGE (When Data Entered)

Block no. 20

rearward-facing steps, cavities and bases. The data which are available are carefully discussed for insights which might be gained regarding probe/cylinder flows. Special emphasis is given to plane-nosed cylinder flows and the opening phenomenon associated with cavity flows.

A simple, semi-empirical free streamline model is developed for the postulated flow field of a low drag probe/cylinder configuration. Partial agreement with inferences from related experimental data is obtained.

The few studies which include transonic flow past probe/cyclinder arrangements are discussed. These studies present conflicting results and hypotheses concerning the reasons for these conflicts are set forth.

ACKNOWLEDGEMENTS

This work was supported by AFOSR Grant 83-0179.

The assistance of Mr. Abdollah Arabshahi and Miss Lisa Willis at Mississippi State University in the literature search and preparation of the figures is gratefully acknowledged. Lt. Bruce Haupt of AFATL/DLCA, Eglin AFB, Florida, participated in many valuable discussions as this work progressed. Lt. Randy S. Buff of the Aeroballistic Research Facility at Eglin AFB provided extremely useful data for this study. Mrs. Rita Curry at MSU quite patiently and ably prepared the final manuscript.

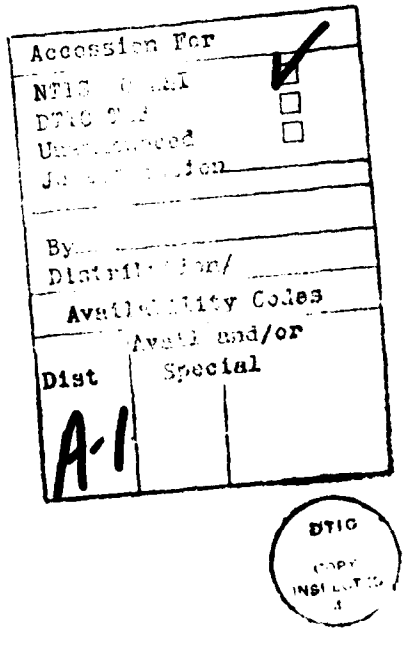

ABSTRACT

An arrangement of a plane-nosed circular cylinder with a smaller diameter plane-nosed cylindrical probe coaxially extending ahead in a transonic axial flow, has been considered. This configuration is a prototype for a low drag forebody replacing more conventional streamlined nose fairings. The open literature contains one study (and, apparently, only one) which clearly shows reductions in transonic forebody drag for such arrangements.

In view of the lack of data on transonic flow past probe/cylinder configurations, an attempt is made to construct the flow field based on data for related and component flows. The flow is modelled as the merging of several component, separated flows. Component flows are axisymmetric plane-nosed cylinders and axisymmetric forward-facing steps. Related flows include rearward-facing steps, cavities and bases. Relatively little data are available in the open literature concerning transonic flow past any of these arrangements, especially for axisymmetric geometries. The data which is available is carefully discussed for insights which might be gained regarding probe/cylinder flows. Special emphasis is given to plane-nosed cylinder flows and the opening phenomenon associated with cavity flows.

A simple, semi-empirical free streamline model is developed for the postulated flow field of a low-drag probe/cylinder configuration. Partial agreement with inferences from related experimental data is obtained.

The few studies which include transonic flow past probe/cylinder arrangements are discussed. These studies present conflicting results and hypotheses concerning the reasons for these conflicts are set forth.

TABLE OF CONTENTS

LIST OF SYMBOLS

Reference quantities are freestream conditions and maximum cross-section diameter.

C_D	drag coefficient
C_p	pressure coefficient
C_{p_b}	base pressure coefficient
C_{p_o}	isentropic stagnation pressure coefficient
C_{p_s}	pressure coefficient on free streamline
d	maximum cross-section diameter
d_1	cross-section diameter of probe or front body
d_2	maximum cross-section diameter
g	gap length between front and rear bodies, length of probe
h	cavity depth, two-dimensional flat plate thickness, step height
	cavity length, probe length
M	Mach number (usually freestream)
p	local static pressure
p_o	isentropic stagnation pressure
p_r	static pressure at reattachment onto closed cavity floor
p_s	static pressure at separation from closed cavity floor
q	dynamic pressure
R_e	Reynolds number
U	freestream velocity
x	streamwise coordinate
x_r	streamwise location of p_r
x_s	streamwise location of p_s

y	coordinate normal to body surface
$(\ )_\infty$	freestream quantity

LIST OF FIGURES

Figures

I. Introduction

Depending on the speed regime, vehicle type and load requirements, various sources of aerodynamic drag exist. Similarly, a variety of ways to minimize this drag; subject to the multitude of other constraints which might exist, have been devised. On a large number of vehicle systems a significant percentage of the aerodynamic drag results from pressures acting on the forebody region of the vehicle main body or fuselage. If the forebody (or nose) is made fairly blunt to optimize volume then a substantial region of near-stagnation pressure exists on the nose; the likelihood of flow separation where the nose transitions to be body sides (that is, at the forebody shoulder) is also enhanced. Near-stagnation nose pressures and forebody flow separation both generally contribute to forebody pressure drag. Vehicles as seemingly unrelated as tractor-trailer trucks and submarine launched intercontinental ballistic missiles are subject to these particular flow problems and are bodies for which the forebody pressure drag can be more than half of the total body drag; see References 1 and 2. Those bodies with substantial forebody drag generally have fairly blunt noses and it is this class of bodies (with basically axisymmetric cross-sections) which this investigation will address.

At subcritical speeds (that is, speeds for which the maximum local Mach number never exceeds one) it is quite possible to maintain a very low value for the drag of blunt forebodies by rounding the shoulder radius, even if the center portion of the nose is still quite blunt. References 3 and 4 present clear examples of this. With proper rounding flow separation at the shoulder can be eliminated and low pressures can

be developed to balance the near-stagnation pressures in the central nose region. At supercritical speeds however, local supersonic flow accompanied by shocks may occur near the rounded shoulders which then negates some of the shoulder radius benefits. The geometries and drag measurements presented in Figure 1 through 4 depict the behavior in these two subsonic freestream regimes. At supersonic speeds detached bow shocks will occur with an accompanying large drag penalty if the forebody is fairly blunt, even if the shoulders are rounded, as shown by the geometries and measurements in Figures 5 and 6 from Reference 5.

A rather unusual but very effective alternative to shoulder rounding exists for reducing blunt forebody drag. Consider a flat-faced cylinder in axially symmetric flow as schematically portrayed in Figures 7 and 8 (from References 6 and 7). At all Mach numbers the flow separates at the face edge and the forebody drag is quite high (C_D based on body diameter is 0.75 or greater depending on the Mach number). The flow field and variation of drag with Reynolds number and Mach number are carefully documented for this problem in References 6, 7 , and 8. Now, suppose for essentially incompressible flow a thin circular disk is coaxially positioned ahead of the cylinder face. As shown in Figures 9 and 10 and fully documented in References 6 and 9, for certain combinations of disk diameter and gap the total forebody drag (disk plus cylinder face) is dramatically low, essentially as low as a carefully streamlined, elongated nose. For supersonic freestreams if the disk is replaced with a thin rod (or spike or probe) similar dramatic drag reductions are obtained (Ref. 10-15). Examples of practical applications of these drag reduction techniques are the drag reduction shields used on tractor-trailer trucks (Ref. 16-21) and the nose spikes

used on the Trident missile (Ref. 2, 15 and 22) and other supersonic bodies (Ref. 23-25). To a certain extent the physics underlying these techniques for drag reduction or drag control at incompressible or supersonic freestream Mach numbers is understood. The important physical property of these flows to note now is that the forward disk or probe causes or induces flow separation and a large region of separated flow is formed. However, here the separated flow is managed in such a way that very blunt bodies can be arranged to have very low drag.

The examples cited above are documented either for low subsonic ($M_\infty < 0.2$) or supersonic freestreams. The situation for transonic freestreams is not so clear. Certainly the problem of transonic drag is important, perhaps even a fundamental limitation in some situations. The present solutions to minimizing transonic fuselage drag center around area-ruling, elongated noses, wing/body blending and simply adding more installed thrust. The concept of using purposely induced flow separation to effectively reduce forebody drag seems to be virtually unexplored. References 2 and 26, with quite limited experiments, dismiss the possibility of transonic drag reduction using induced separation although these references clearly show the effectiveness of such an approach at supersonic speeds. Spooner, in Reference 27 on the other hand, demonstrates that induced forebody flow separation can substantially reduce transonic forebody drag. This paper, unfortunately, is also quite limited in the situations it considers and thus can only serve as a hint as to what might be possible. Nevertheless, the evidence given by Spooner establishes that induced flow separation can be exploited in the transonic flow regime.

II. Merging Separated Flows

The physical explanation for reducing forebody drag using induced flow separation can be thought of in perhaps several ways. One view, which might provide the best approach for transonic problems, is to consider the flow field as the result of the merging of several distinct separated zones. This particular approach allows certain geometric criteria to be established that would be an aid in predicting low drag configurations.

Consider first the subsonic disk/cylinder configuration. The cylinder by itself has a large separated region extending downstream from the cylinder face edge (Figures 7, 8 and 9). A disk by itself and normal to the flow also has a large separated region or wake extending downstream from the disk edge. When a cylinder is introduced behind the disk the disk wake interacts or merges with the cylinder flow. For certain arrangements the interaction is such that the separated zone of the cylinder disappears, or equivalently, the disk separation merges smoothly onto the cylinder sides as sketched in Figures 9c and d. This situation has the lowest forebody drag as depicted by Figure 10 which presents selected results from Reference 6 for the forebody drag coefficent of disk/cylinder combinations. Pressure measurements reveal large negative pressure coefficients near the outer radius of the cylinder face and these low pressures balance the near-stagnation pressures on the disk face. For the optimum arrangements, turbulence measurements also show very low shear stress in the shear layer spanning the disk to cylinder gap, a phenomenon which is consistent with the observed low drag force (Ref. 6). In any case, the optimum (lowest drag) situation is when the separation surface from the disk merges

smoothly onto the cylinder and eliminates the cylinder separation. Although it is not within the scope of the present study, it should be noted that the optimum axisymmetric geometries can be predicted with reasonable accuracy using axisymmetric, potential flow free streamline theory as developed in References 6, 28 and 29. It should also be re-emphasized that the total forebody drag at optimum is on the same order as a well streamlined solid forebody; this is a rather startling and unexpected result.

A very extensive body of literature, such as References 2, 10-15, 22-27, and 30, exists regarding the use of induced flow separation to reduce the drag of blunt bodies in supersonic streams. A brief summary of the most important points relative to forebody drag follows. If a spike is extended coaxially ahead of a flat-faced cylinder, say, in supersonic flow a conical shock will usually form at the spike tip. The pressure rise across this conical shock may cause the boundary layer on the spike to separate and form a nominally conical shaped region which, for the proper length and diameter spike, will merge smoothly onto the cylinder (Fig. 11a). The separated zone gives the cylinder an effectively conical nose with low drag. Depending on the length and diameter of the spike other flow fields with multiple separations are possible such as indicated in Figure 11b for a very long spike. The lowest drag is apparently obtained for the longest spike which has a single separated zone from the spike tip to the cylinder edge (Ref. 30). That is, for the least drag the various possible separations have just merged into a single separated region. The conical nature of these supersonic flow fields lends itself to a partial analytical treatment in terms of predicting the flow geometry. Examples of this analysis are

given in Refereces 10 and 30.

We have thus far seen that using induced flow separation to reduce blunt forebody drag is well documented and is related to forming a single separated flowfield from multiple separated regions. Also we have noted that for low subsonic and supersonic freestreams, at least, some of the analysis to predict these flows can be done with relatively well understood and developed techniques--potential, free streamline flow for the subsonic case and conical flow for the supersonic problem. Modern computational fluid dynamic codes would presumably yield better predictions, for example References 31 and 32, although they will encounter turbulence modelling problems (as do the analytical methods for that matter). For transonic flows one would expect that there should be some qualitative physical similarities to the subsonic and supersonic cases in terms of producing a single separated zone from multiple separations to yield a low drag configuration. A hypothetical situation is shown in Figure 12. In part (a) of this figure a blunt-faced cylinder in supercritical but subsonic flow is shown without a drag reduction probe or device in front. (This figure is based on unpublished experimental results in Reference 33). A large separated zone develops at the cylinder face edge while further aft a shock forms. Now suppose a moderate diameter, long cylindrical probe is extended in front as shown in Figure 12b. Three separated zones most probably would appear accompanied by shock waves. A similar flow should develop in low subsonic flow but without the shocks. Stagnation pressure on the probe face and elevated pressures at the reattachment points on the cylinder face would give this configuration substantial drag although probably not as much as would be encountered in Figure 12a. If this probe is

progressively shortened it is likely that a flow field as shown in Figure 12c would form where the two probe separations have merged and faired smoothly onto the cylinder sides thereby eliminating the third separated zone. The longest probe length to give this flow would probably have the least drag, although this will depend on Mach number and Reynolds number, the probe diameter and the shape of the probe face (flat, ogive, etc). However the qualitative flow features should be essentially the same as described. If the freestream Mach number is slightly supersonic, a detached nearly normal bow shock would form and the qualitative features as described should still occur.

There are several serious difficulties associated with assessing the validity of the transonic flows postulated above. To the author's knowledge, there exist in the open literature no thorough flow field measurements nor flow visualizations of the transonic probe/cylinder flows. Similarly, no analytical or numerical tools exist which are capable of calculating these flows which would have to be regarded as large disturbance transonic flows. (Such large separated regions are beyond the scope of the most sophisticated Navier-Stokes codes on the largest machines). Without experimental results or calculational methods available for this problem, any attempt to predict the geometries which are most likely to give low drag probe/cylinder combinations in transonic flow must rely on modelling the flow based upon results for related geometries. Even here, as will be seen, truly appropriate and useful information is essentially lacking, at least in the open literature. Consequently verifying the postulated flows and predicting low drag geometries is, at this time, an extremely tenuous and suspect proposition.

Before any further development is undertaken let us briefly review the overall problem. An important aspect of vehicle design is the compromise between volumetric efficiency, that is large, useful interior volume and aerodynamic efficiency, or drag. Large, useful volumes imply blunt-nosed bodies. One technique for reducing the drag of blunt bodies is to induce flow separation ahead with a disk, spike or other device. The feasibility of such a technique has been amply demonstrated and is in regular use for low subsonic and supersonic vehicles. The questions here are whether such a technique is feasible at transonic speeds and what geometrical arrangements would yield the lowest drag. This leads to the need to understand the nature of various separated transonic flows which brings us to the discussions to follow.

III. Component and Related Flows

Referring again to Figure 12, three separated regions possibly exist and these may be considered to be component flows from which a model for predicting low drag geometries might be developed. As shown in Figure 12b, the probe is a flat-faced circular cylinder in axial flow (other geometries for the probe face could also be used). The separation from the probe face eventually reattaches and forms what is presumably a turbulent boundary layer on the probe sides. The probe boundary layer then encounters the face of the main body, this encounter essentially being an axisymmetric forward-facing step flow. The probe boundary layer separates under the influence of the step adverse pressure gradient and reattaches somewhere on the main cylinder, here shown on the main cylinder face. A third separation then might occur at the edge of the main cylinder face. The principal elements, or components, of this situation are then axial flow past a flat-faced cylinder plus turbulent flow approaching an axisymmetric forward-facing step.

As the probe is progressively shortened the separation from the probe face will eventually merge with the forward-facing step separation to form presumably a single separated zone as depicted in Figure 12c. The transition from the situation in Figure 12b to that in Figure 12c is quite reminiscent of the process of cavity opening as first defined by Charwat, et. al. in Reference 34. Axisymmetric cavity opening then might serve as the prototype for the merging of the separated flows to form the low drag configuration.

To model the transonic flow past a probe/cylinder combination, it thus appears that the important information to have concerns the flow

field properties of (1) flat-faced cylinders in axial flow, (2) axisymmetric forward-facing steps and (3) axisymmetric cavities, each of these in transonic freestreams. A very careful study of the open literature has revealed only data concerning the first flow, that is the flat-faced cylinder in an axial, transonic freetream which appears in Stanbrook's study, Ref. 35. One other source of relevant information is Reference 15 where pressure distributions are given for a probe in front of a blunt (although rounded) nose. In this report (Ref. 15) however only data for one configuration is shown which greatly limits the usefulness of the information.

A group of somewhat related papers exist which provides some insight into the flow processes and these will be briefly reviewed here. A landmark paper concerning the conditions for separation of a boundary layer encountering an obstacle is the work by Chapman, et. al., Reference 36. This paper concerns transonic and supersonic freestreams approaching two-dimensional obstructions and the emphasis, as the paper's title implies, is on the effect which the location of laminar to turbulent transition has on the separation and reattachment of various separated flows. Direct application of this work to the present problem is limited because the flows studied by Chapman are essentially two-dimensional and primarily supersonic. A similar landmark work is that of Charwat, et. al., Ref. 34 which has previously been mentioned. This paper deals with primarily supersonic, two-dimensional cavity flows with emphasis on the cavity opening process. Again, the supersonic, two-dimensional aspects of the flows in Reference 34 limit its applicability to the current problem. One additional difficulty is that cavity flows such as Charwat considers have the initial orientation of

the separation streamline (or surface) essentially parallel to the freestream whereas, in the current problem the flow initially separates with a direction 90 degrees to the freestream (that is, the flow separating from the probe face). Wu, et. al., Ref. 37 also provide detailed measurments for two-dimensional cavities and forward-facing steps, with much information at transonic speeds. However there appear to be various inconsistencies and errors in this work which, when coupled wtih the fact that it is two-dimensional, limits its usefulness. Three-dimensional cavities at transonic speeds are the concern of Rossiter in Reference 38 and this paper does provide some useful guidelines although it is still restricted because the flow is not axisymmetric and the separation is parallel to the freestream.

As previously mentioned, information on probes ahead of blunt noses in supersonic freestreams is relatively abundant. At lower supersonic Mach numbers, four references in particular are useful. Beastall and Turner, Ref. 12, present some of the first detailed observations of the use of probes as drag reduction devices and include some pressure distributions on the main body face. An even earlier work by Mair, Ref. 11, provides good flow visualizations but no flow field measurements. Moeckel in Reference 10 develops an analytical description of the conical flow field created by the tip shock and separation although his analysis ultimately requires knowledge of the turbulent shear properties of the shear layer between the separated and unseparated flow. These turbulent properties are still essentially unavailable. Finally, Zorea and Rom, Ref. 30, develop semi-empirical relations for low drag supersonic probe configurations which are apparently valid for freestream Mach numbers between 1.5 and 3.0. Each

of these references is useful to some extent but all are supersonic and either do not present sufficient detailed measurements or are based on conical flow assumptions and thus have limited usefulness for the transonic problem.

A useful companion to the supersonic two-dimensional cavity studies of Charwat, et. al., Ref. 34, and Rossiter, Ref. 38, is the work by Johannesen in Reference 39 on supersonic annular (or axisymmetric) cavities. Although this work is supersonic it does present detailed pressure distributions for closed and open cavities and provides a means to relate, in some way, two-dimensional observations to analogous axisymmetric configurations. A paper by Roshko and Thomke, Ref. 40, deals with supersonic axisymmetric rearward-facing steps and also provides information which would be useful in relating axisymmetric and two-dimensional flows. Merz et. al. in Reference 41 consider transonic axisymmetric base flows and this paper provides useful information on the relations between conditions at separation and the properties of the separated region, although the particular configuration is not directly the same as the current problem. Finally, Ericsson and Reding, Ref. 42, in their review of support interference effects (an example is Reference 43) present limited information on the influence of downstream obstacles on separated flow at a variety of Mach numbers. This paper is most closely related to the axisymmetric cavity problem, however.

The papers summarized here constitute the effective fluid mechanic data base from which a model for the axially-symmetric, transonic, probe/cylinder flow might be developed. This data base is, in reality, insufficient for a realistic and verifiable model to be formed. Perhaps the most important conclusion which can be drawn from

this survey is that significant experiments and analyses are necessary before any true assessment of the potential for drag reduction using induced flow separation can be made. Of course it should be re-emphasized that the work of Spooner, Ref. 27, establishes that significant drag reductions are possible. However his paper, which is limited to one probe configuration and only net forces, does not supply sufficient information for modelling or predictions.

IV. Free Streamline Model for Probe/Cylinder Transonic Flows

Along the boundary of a large separated flow region it is often appropriate, or at least assumed, that the pressure is constant. This type of flow is referred to as a free streamline flow. It is proposed here that for low drag probe/cylinder configurations the flow separates from the face of the blunt probe and reattaches smoothly onto the sides of the cylinder as shown in Figure 12c. Let us consider the separated streamsurface here to be a constant pressure surface with a pressure coefficient C_{ps}, which is generally negative. We then have a free streamline problem for the shape and size of the separated zone, (Fig. 13).

Several approaches might be taken in addressing this free streamline problem. References 28 and 29 give incompressible, potential flow solutions for axisymmetric free streamlines. Both approaches are quite complicated. Let us here take a less involved approach. Kuchemann and Weber, in their classic text on propulsion, Reference 44, derive the shape of optimum circular intakes for incompressible flow where the outer surface is a constant pressure surface, as depicted in Figure 14. One result of their derivation (Equation 4-6 in Reference 44) expresses the ratio of the maximum cross-sectional area of the outer surface A_m to the inlet area A_i. This is analogous in the present case to the ratio of the cylinder frontal area to the probe frontal area, A_2/A_1. Their result is, for incompressible flow

$$A_m/A_i = 1 + \frac{(1 - V_i/V_o)^2}{(V_m/V_o)^2 - 1} = 1 - \frac{1}{C_{ps}}(1 - V_i/V_o)^2 \qquad (1)$$

where the velocities V_o, V_i and V_m are the freestream, intake and maximum outer surface velocities respectively. C_{ps} is the (constant) outer surface pressure, $1 - (V_m/V_o)^2$. For no intake velocity (analogous to blocking the intake or having a solid probe face occupying A_i) then

$$A_m/A_i = A_2/A_1 = 1 - 1/C_{ps} \tag{2}$$

Kuchemann and Weber also develop a semi-empirical relation for the ratio of the maximum outer diameter to the intake length, D_m/L, in terms of the same velocities as in equation (1) for an optimum intake. This result (incompressible, Equation 5-7 from Ref. 44) is

$$D_m/L = 7.8(1 + 0.4(V_i/V_o)^2) * (V_m/V_o - 1) \tag{3}$$

where the factors 7.8 and 0.4 were empirically determined by Kuchemann and Weber. For $V_i = 0$ and letting d_2 and ℓ replace D_m and L we have

$$d_2/\ell = 7.8(V_m/V_o - 1) = 7.8((1 - C_{ps})^{1/2} - 1) \tag{4}$$

Equations (2) and (4) now yield expressions for the required incompressible probe/cylinder geometry, that is d_1/d_2 and ℓ/d_2, given a free streamline pressure. This assumes, of course, that a free streamline and a solid body will have the same shape if the pressure along each is the same constant value.

For compressible flow, corrections must be made to these relations. Although the flat probe face acts as an abrupt and large disturbance to the flow it might be assumed that the free streamline

surface is itself a significantly smaller disturbance and that the linearized subsonic similarity rules might be roughly applicable. Therefore, following Chapter 5 of Schlichting and Truckenbrodt, Ref. 45, the transformation from the incompressible fuselage to an equal length compressible fuselage (the Prandtl-Glauert-Goethert-Ackeret rule) is:

$$R_{inc} = R(1 - M_{a\infty}^2)^{1/2} \qquad \text{(Equation 5-52a, Ref. 45)}$$

$$C_{p_{inc}} = C_p(1 - M_{a\infty}^2)^{1/2} \qquad \text{(Equation 5-53, Ref. 45)}$$

where R refers to radius, $M_{a\infty}$ is the freestream Mach number, the subscript 'inc' refers to the incompressible problem and no subscript refers to the equivalent compressible problem.

Equations (2), (4), (5) and (6) can be used to express the properties of the compressible probe/cylinder flow in terms of the parameter V_m/V_o which is now somewhat artificial since it refers to an incompressible flow.

First we note from (2) and (5) that

$$d_2^2/d_1^2 = 1 + \frac{1}{(V_m/V_o)^2 - 1}$$

or

$$d_1/d_2)_{comp} = \left(1 + \frac{1}{(V_m/V_o)^2 - 1}\right)^{-1/2} = \frac{((V_m/V_o)^2 - 1)^{1/2}}{V_m/V_o} \qquad (7)$$

From (4) and (5) we have, letting $M_{a\infty} = M_\infty$

$$d_2/\ell_{inc} = (d_2/\ell)_{comp} * (1 - M_\infty^2)^{1/2} = 7.8\ (V_m/V_o - 1)$$

or

$$\ell/d_{2_{comp}} = \frac{(1 - M_\infty^2)^{1/2}}{7.8(V_m/V_o - 1)} \tag{8}$$

And finally the definition of V_m/V_o and (6) give

$$C_{ps} = \frac{1 - (V_m/V_o)^2}{(1 - M_\infty^2)} \tag{9}$$

Equations (7) through (9) describe the subsonic compressible probe/cylinder flow as follows. A free stream Mach number, M_∞, is first selected then equations (7) and (8) can be used together to plot ℓ/d_2 versus d_1/d_2 by varying the parameter V_m/V_o. Equivalently V_m/V_o can be eliminated from this pair of equations and ℓ/d written directly as a function of d_1/d_2 with M_∞ as a parameter. A similar procedure is followed with equations (7) and (9) to obtain C_{ps} as a function of d_1/d_2 and M_∞ (either through the parameter V_m/V_o or directly). Selected plots of ℓ/d_2 and C_{ps} versus d_1/d_2 with M_∞ a parameter are shown in Figure 15. Notice how the streamline pressure becomes more negative and the probe becomes shorter as the probe diameter is reduced. These trends are consistent with experimental results of incompressible flow as given in Reference 6.

The assumptions and limitations of the preceeding derivation should be restated. They are as follows:

1. Low drag compressible probe/cylinder configurations have a

single separated zone.

2. The pressure along the boundary of this separation is essentially constant.

3. A solid surface and a free streamline both with the same constant pressure have essentially the same shapes.

4. The Kuchemann-Weber derivations for the area ratio and diameter to length ratio apply to the probe if the intake velocity, V_i is zero.

5. The Kuchemann-Weber relation for diameter to length ratio contains empirical constants whose values and invariance in a compressible flow are not established.

6. The subsonic similarity rules for transforming from an incompressible to a compressible are valid for $M_\infty < 1$, and strictly, $M_{max} < 1$.

7. The free streamline surface can be at least approximately treated using linearized potential flow.

Confirmation of both the qualitative and quantitative validity of this free streamline model must await further developments.

V. Some Observations from Previous Experiments

A. Transonic probes

Primarily two experiments form the data base for the effects on transonic drag of probes extended in front of blunt bodies. The early work of Spooner, Ref. 27, provides the motivation for pursuing this method of drag reduction. A portion of Spooner's results have been collected and plotted in Figure 16 in a form which more clearly shows the drag reduction potential than Spooner's original report. Figure 17 shows the drag coefficient of the entire body (not just axial force coefficient) versus angle of attack for the simplest of Spooner's bodies (shown in the inset) with and without a probe. This figure clearly shows that for Mach numbers between 0.8 and 1.2 and angles of attack up to 10 degrees the probe significantly reduces the drag of the entire body. The transonic drag rise is greater with the probe as shown in Figure 16 for zero incidence but the overall values of drag coefficient are still considerably less with the probe. It should be noted that, in general, the transonic drag rise for low drag bodies is proportionally greater than the drag rise for high drag bodies as described in Reference 46.

As a contrast Figure 18 presents some measurements of the influence of a probe on the forebody drag of a more rounded body, from Reference 2. No drag reduction is indicated for subsonic Mach numbers with the probe extended although substantial reductions are obtained in supersonic freestreams. Several factors must be remembered when viewing this figure. The body even without a probe has relatively low subcritical forebody drag. A probe would not necessarily be expected to

help much. In addition, only one probe geometry (shown in the inset) is presented here. It is conceivable that a different arrangement might provide some transonic drag reduction. A very cursory investigation, Ref. 26, also shows no transonic drag reduction due to a probe. This report suggests that the problem involves flow oscillations but does not provide sufficient information to be in any way conclusive.

No other published references showing the explicit effects of a probe on axisymmetric blunt forebodies in transonic freestreams are known to the author. One set of results from presently unpublished preliminary experiments (Ref. 33) of ballistics tests of bodies with large diameter probes is shown in Figure 19. The configurations explored are shown in part a of this figure. The drag coefficient, C_D, is for the entire body. This figure shows that addition of a probe decreases the overall drag and that an optimum probe length probably exists for each basic body and probe diameter. Insufficient data are available from these experiments to draw any more significant conclusions.

B. Flat-faced circular cylinders

As was described in Section III of this study an important component flow of the probe/cylinder problem is axial flow past a flat-faced circular cylinder. The variation of drag coefficient of the face as a function of Mach number is thoroughly discussed by Stanbrook in Reference 7 (also see Koenig, Ref. 6). Stanbrook presents empirical expressions for the drag of the flat-face as follows:

$$C_D = 0.758 + 0.296\ M_\infty^2 \qquad \text{for } M_\infty < 0.9$$

$$= (0.9054\ p_{o_2} - p_\infty)/q_\infty \qquad \text{for } 0.9 < M_\infty < 1.5$$

where p_∞, q_∞ and M_∞ are freestream values of static pressure, dynamic pressure and Mach number, respectively, and p_{o_2} (or p_{t_2}) is the stagnation pressure behind a normal shock. Hoerner, Ref. 47, writes the forebody drag as

$$C_D = 0.74\ (1 + 0.25\ M_\infty^2) \text{ over the transonic regime.}$$

The important points to notice from these empirical results are that the drag is high even for $M_\infty \to 0$ and that the drag increases as M_∞^2. Further elaborating on this second point, the stagnation pressure coefficient of the freestream is

$$C_{po} = \frac{p_{o_\infty} - p_\infty}{\frac{\gamma}{2} p_\infty M_\infty^2}$$

and Stanbrook's correlations (Fig. 20 here, Fig. 3 from Ref. 7) show that $C_D \doteq C_{po} + 0.2$ over a freestream Mach number range of 0 to at least 2.6, which makes an extremely useful rule of thumb for estimating blunt nose drag.

Another paper by Stanbrook, Ref. 35, provides an important set of pressure measurements on flat-faced circular cylinders at transonic and supersonic Mach numbers. Some of his results, in a slightly different format, are presented in Figure 21, where the distribution of wall static pressure coefficient along the cylinder side is given for various freestream Mach numbers. Notice that in the initial separation just

downstream of the cylinder face the pressure coefficient is roughly constant at a value around -0.44. Stanbrook notes that for freestream Mach numbers greater than about 0.8 the flow on the cylinder face just at the edge is sonic which accounts for the relative invariance of the initial pressure distribution with Mach number. A rapid recompression follows and the pressure coefficient reaches a maximum value on the order of +0.08. Recovery to the freestream pressure then occurs. In Figure 22 selected pressure distributions are superimposed upon sketches of shadowgraphs from Reference 33; an indication of the relation of the pressure distribution to the flow field can be seen.

The axial location of the maximum pressure location might be taken as some measure of the length of the separated zone for this type of flow. As has been well discussed by many experimenters (Ref. 36 for example) true reattachment occurs upstream of the maximum pressure location. However, the maximum pressure is easy to locate and at least should give a relative indication of the separated zone length. This length is probably an important parameter which influences the probe length at which the probe/cylinder flow changes from multiple separated zones to a single zone. Figure 23 presents the length to maximum pressure versus Mach number for flat-faced circular cylinders. The data here comes from References 8, 11, 12 and 35. A peak near $M_\infty = 1$ is obvious and might be expected. Interestingly, flow visualization (Fig. 22b) indicates that the lateral extent of the separated zone is relatively small for $M_\infty = 1$. This suggests that the location of maximum pressure is only a rough measure of the extent of separation. Considerable recompression may be occuring in the developing reattached boundary layer.

Ota, in References 8 and 48, explored the separated region created by a plane-nosed cylinder and a blunt flat plate in very low Mach number flow. Several important results from these studies are presented in Figure 24 and Table 1. The pressure coefficient distributions show the two-dimensional flat plate flow to have a more negative value in the separated region than the axisymmetric flow although the difference is not as great as might be expected. The length of the two-dimensional separation bubble is significantly greater, however, than the axisymmetric bubble length. Another important result from Ota's studies is that, for low Mach numbers at least, the location of maximum pressure on the sides of both bodies is actually quite close to the reattachment location found using tuft probes or skin friction measurements. This provides some justification for the use (Figure 23) of the location of maximum pressure as a measure of the extent of separation for flat-faced cylinders.

C. Base and rearward-facing steps

There is an abundance of data available on base flows for a wide variety of geometries. Merz, et. al., in Reference 41 present a comprehensive survey of subsonic and transonic axisymmetric base flows along with extensive measurements of their own. A rearrangement of a portion of their results is presented here in Figure 25 where the length to reattachement (or closing) of the base wake is plotted against base pressure coefficient with increasing subsonic Mach number indicated. The wake closure length increases with more negative base pressure coefficients and also with increasing free stream Mach number. These trends are similar to the behavior of the separated zone near the nose

of a flat-faced circular cylinder, shown previously in Figures 21 and 23. For the nose separation region the distance to maximum pressure increases with increasing subsonic free stream Mach number. Also the pressure at separation on the nose tends to be slightly more negative for higher values of Mach number. This is in contrast to one of the predictions from the simple free streamline approach presented earlier (Fig. 15). The free streamline analysis indicates that the separated zone becomes shorter, not longer, as the pressure coefficient becomes more negative and also as the Mach number increases for a given probe/cylinder diameter ratio. The reason for this difference is not yet clear. There is agreement, however, between the analysis and experiment for the variation of separation pressure coefficient with Mach number. For all three cases, the pressure coefficient becomes more negative as the free stream Mach number becomes greater.

An informative comparison between two-dimensional and axisymmetric base flows is shown in Figure 26 taken from Reference 49. The two-dimensional base in transonic flow has considerably more negative pressure than the corresponding axisymmetric situation. Here the three-dimensional relief available for flow past the axisymmetric geometry is especially strong near $M = 1$. It is reasonable to suppose that a similar situation would exist for a comparison of a blunt-nosed cylinder and flat plate.

Flow past a rearward- or downstream-facing step is closely related to base flows. There are numerous papers concerning two-dimensional rear steps and covering a broad Mach number range, e.g., References 50 and 51. Studies of axisymmetric rear steps, especially in the transonic regime, are relatively scarce however.

A comparison of supersonic turbulent flow past a two-dimensional and an axisymmetric rear step (data from References 36 and 49, respectively) is shown in Figure 27. The axisymmetric step has higher pressures (and thus less negative pressure coefficients) down stream than for the two-dimensional case. This is in keeping with the three-dimensional relief available for the axisymmetric flow and is consistent with the results in Figure 26 for base flows and in Figure 21 for nose separations. The axisymmetric pressures overshoot the free stream pressure however and require considerable downstream distance before they eventually recover to the proper inviscid flow value; the recovery is not shown in the figure. The two-dimensional pressures, on the other hand, montonically recover to the free stream value in a relatively shorter distance.

Reference 52 by Chapman is a thorough and often-cited study of supersonic base flows including the effects of a downstream support (which effectively forms a rear step). For the present investigation one very important result from his work is to be noted. Chapman investigated a wide variety of geometries with both laminar and turbulent separations over large Mach number and Reynolds number ranges. For all situations the base pressure coefficient was negative and nominally between -0.1 to -0.2. Only when the rear support became equal in diameter to the base diameter (thus eliminating the base) did the pressure coefficient significantly increase, and then only to 0.0, never a positive value. This result will be referred to later.

D. Cavities

Flow over a cavity or cutout in a surface takes one of two forms.

As first defined by Charwat, Ref. 34,. a cavity is termed 'open' if the initial separation streamline completely spans the cavity and reattaches onto the downstream wall. The cavity is considered 'closed' if the separation from the upstream cavity wall reattaches to the cavity floor with a second separation occurring ahead of the downstream wall. An open cavity is analogous to the single merged flow field proposed for the low drag probe/cylinder geometry as suggested in Figure 28. The conditions for 'opening' of a cavity are, therefore, of particular relevance to the probe/cylinder flow problem.

References 34, 37, 38 and 39 discuss experimental studies of cavity flows which are particularly applicable to the present problem. The important experimental parameters of these four studies are given in Table 2 while Figures 29 through 34 present comparisons and rearrangements of some of the results.

The transition from a closed to an open cavity is nicely depicted by the succession of cavity floor pressure distributions in Figure 29 which is taken from Reference 39. This axisymmetric cavity is being progressively shortened (viewing the figure from bottom to top) with the approach flow conditions and the depth held constant. At the longest gap (/h = 16) the flow separates from the corner of the rearward-facing step with a pressure coefficient of about -0.17. This first separation reattaches to the cavity floor at about x/h = 4 with an accompanying pressure rise up to C_p = +0.05. The flow progresses along the cavity floor with a very slight decrease in pressure until it encounters the influence of the forward-facing step. A second separation occurs at approximately x/h = 12 with an accompanying press e rise, a short constant pressure plateau and a further pressure

rise to reattachment (with C_p = +0.4) onto the forward-facing step. Thus, two very well defined separated zones are present for this closed axisymmetric cavity flow.

When the cavity is shortened to ℓ/h = 10.4 the pressure distribution retains most of the qualitative and quantitative features seen in the flow for ℓ/h = 16 although the reattachment from the downstream-facing step and the separation ahead of the upstream-facing step have become close together. An important difference between the ℓ/h = 10.4 and 16 flows is that for the shorter cavity the pressure along the central portion of the floor, after reattachment, continues to increase whereas the longer cavity shows a slight decrease. The cavity at ℓ/h= 10.4 is still closed but the two separated zones are less distinct and have nearly merged.

Further shortening the cavity to ℓ/h = 8 produces a pressure distribution which differs both qualitatively and quantitatively from the longer cavity distributions. The pressure coefficient at separation is significantly increased to C_p = -0.02. A slight decrease in pressure then occurs followed by a weak continuous recompression to a reattachment value on the forward-facing step of +0.13. This cavity has opened and the distribution shown is characteristic of nearly all open cavities.

The other distributions in Figure 29 essentially display the features of the neighboring distributions selected for discussion. For ℓ/h = 12, the distribution is virtually identical to ℓ/h = 16, except that the central attached flow region is shorter. At ℓ/h = 9.6 the distribution is similar to ℓ/h = 8 although the separation pressure for ℓ/h = 9.6 is more negative and there is 'bump' in C_p (due to a

secondary vortex) shortly after the initial separation. From the text of Reference 39, the cavity was determined to open at $\ell/h = 10$ so this distribution ($\ell/h = 9.6$) has just opened. The distributions for $\ell/h < 8$ are basically like that for $\ell/h = 8$ although for the shortest cavity the reattachment pressure coefficient is only zero.

The sequence of pressure distributions in Figure 29 provides several suggestions for criteria for cavity 'opening'. One criterion might be that the cavity will open when the pressure at reattachment from the rearward-facing step becomes equal to the pressure at separation ahead of the forward-facing step. Another criterion might be that the cavity opens when the pressure coefficient at the initial separation (i.e. of the rearward-facing step) becomes approximately zero, as compared to the relatively large negative value for a closed cavity. The pressure at reattachment on the forward-facing step might also serve as a criterion since it drops to a relatively low value when the cavity opens.

The situation considered in Reference 39 and shown in Figure 29 is for a supersonic flow past an axisymmetric cavity. Pressure distributions for two-dimensional and rectangular cavities in very low subsonic through transonic freestreams such as presented in References 38 and 53 are very similar to those in Figure 29. Cavity opening for these cases also occurs for ℓ/h near 10. It might then be concluded that the basic character of cavity flow, at least in terms of the shape of the mean pressure distributions and the critical length for cavity opening, is relatively independent of cavity geometry and freestream Mach number.

The work by Wu, et. al., in Reference 37 is an extensive

collection of measurements concerning long, closed two-dimensional cavities in subsonic and transonic flow. Portions of the results from Reference 37 has been rearranged to form Figures 30 and 31. Here the ratio of reattachment pressure (from the rearward-facing step) to free stream pressure p_r/p_∞ and the corresponding ratio for the separation pressure ahead of the forward-facing step p_s/p_∞ are plotted against cavity length to depth ratio ℓ/h with freestream Mach number constant. Using the notion that cavity opening corresponds to a merging or equality of p_r and p_s, gives the results that for $M_\infty = 0.6$ (Fig. 30) the cavity should open at ℓ/h 8.5. This is somewhat shorter than what has been observed in other studies and also shorter than what the authors of Reference 37 consider to be the critical length ($\ell/h \simeq 10.5$). Nevertheless it is clear that, for $M_\infty = 0.6$ at least, p_r and p_s approach the same value shortly before the cavity opens. Figure 31 is a similar plot for $M_\infty = 0.8$ and 0.84. Much less data are available in Reference 37 for these values of M_∞ and so this figure is rather incomplete. For $M_\infty = 0.84$, p_r and p_s are coverging as ℓ/h decreases; extrapolation to equal values for p_r and p_s gives a very short, $\ell/h \simeq 5$, critical length however. The data for $M_\infty = 0.8$ do not appear to converge. The reason for this is unclear. It must be noted that a number of minor errors and inconsistencies have been found in Reference 37 and so the behavior indicated in Figure 31 may not be quite accurate. However, it is probably reasonable to say, based on $M_\infty = 0.6$ and 0.84 in Figures 30 and 31 that p_r approaching p_s is a reasonable measure of cavity opening as ℓ/h decreases.

The work by Charwat, et. al., Ref. 34, is an extremely important study of cavity flows. As mentioned previously, this paper defines the

terms 'open' and 'closed' with regard to cavities and explores the conditions for cavity opening for a wide variety of situations (although some in a very cursory manner) including two-dimensional and axisymmetric flows, free wake/body interactions and cavities in both subsonic and supersonic streams. The bulk of the data presented in this paper, however, is concerned with two-dimensional, supersonic cavity flow.

For the interests of the present study there is one particularly important result from this paper. Charwat concludes that the critical separation length for cavities (ie. the cavity length at which the cavity changes from closed to open) is roughly 12 cavity depths or $\ell/h = 12$, independent of Mach number and geometry. In other words, subsonic or supersonic flow past two-dimensional or axisymmetric cavities will change from the closed mode to the open mode as ℓ/h decreases to below 12, aproximately. It must be emphasized that Charwat's conclusion is based on a limited amount of data, particularly for axisymmetric and subsonic flows. In the earlier discussions of Johannesen's study of supersonic, axisymmetric cavities, Ref. 39, and the work of Wu, et. al., Ref. 37, on transonic two-dimensional cavities, it was noted that these authors observed opening at a value of near 10 for ℓ/h. It is perhaps best to set the length for cavity opening as between 10 and 12 cavity depths in view of all of the available data. But the main point from Charwat's work, that the length is relatively insensitive to Mach number and geometry, is still basically valid and is quite an useful result.

Selected results from Charwat's work are compared in Figures 32, 33 and 34 with the results from Wu, Rossiter (Ref. 38), and Johannesen.

The common feature of each of the data sets is that the value of ℓ/h is between 8 and 12, that is near closure. These three figures then depict some of the difference in the cavity wall pressure coefficient distributions which arise from different freestream Mach numbers and geometries. Figure 32 shows that there appears to be a significant difference in the level of pressure in the downstream half of the cavity for subsonic and supersonic flow. In Figure 33 the comparison is between subsonic flow past a two-dimensional cavity (Charwat) and a three-dimensional, rectangular cavity (Rossiter, Ref. 38). Very little difference is noted; this can also be seen in the previous figure for supersonic flow. Finally, Figure 34 compares supersonic flow past a two-dimensional cavity (Charwat) and an axisymmetric cavity (Johannesen). The shapes of the distributions are qualitatively similar but the axisymmetric cavity has a much greater change in pressure from the initial separation to the final reattachment. This is most probably because the two-dimensional cavity is near opening while the axisymmetric cavity is still closed. This shows that $\ell/h = 12$ is not a precise, universal value for the critical cavity length.

One more result from these cavity flow studies and also that of Roshko, Reference 53, (which concerns very low Mach number streams past rectangular cavities) should be noted. In each case where data were obtained for both closed and open cavities, the pressure coefficient immediately after the initial separation was roughly -0.1 when the cavity was closed and became approximatley zero when the cavity opened, roughly independent of Mach number and geometry. Thus this pressure can serve as an indicator of cavity opening. It should also be noted that this pressure coefficient was never observed to have an appreciable

positive value. Similar behavior for base flows, especially from Reference 52, was commented on earlier in the present study.

To conclude this discussion of cavity flows, some cautions should be made. The characteristics of the boundary layer at the initial separation are important parameters in this problem (Chapman, Ref. 52, Gharib, Ref. 54). These characteristics are not the same for the various stuies cited here and the generalizations made here are thus to be regarded as tentative, subject to difference in the boundary layer properites. Also,the emphasis has been on mean cavity pressures. The flow, in fact, is highly unsteady for certain freestreams and cavity geometries and this also will limit the applicability and usefulness of these conclusions as observed by McGregor and White in Reference 55. Finally, the direction of the flow at the initial separation is parallel to the freestream whereas for a flat-faced probe ahead of a flat-faced cylinder the initial separation is perpendicular to the freestream. This may have a significant effect on the actual values of pressure coefficients and critical lengths which apply to probe/cylinder. Evidence for this is given in Reference 6, for example, where disk/cylinder geometries have critical lengths more on the order of five, rather than ten as observed in the parallel separation cases.

E. Trident missile nose spike

The studies made concerning the Trident missile drag reduction nose spike (Refs. 2, 15 and 2) include a few measurements of the pressure distribution along with the spike and forebody for transonic freestream Mach numbers. The published data, presented here along the geometry in Figure 35, are for only one spike length and diameter, and

are, in fact, the only flow data which were found in the present investigation for drag reduction spikes at transonic speeds.

In examining the pressure distributions of Figure 35 one notes that, except for a small central portion of the spike at the lowest Mach numbers shown, the pressure coefficient is everywhere positive. This is somewhat surprising. One would expect, at least very near the base of the small front disk where the flow initially separates, that the pressure coefficient should be negative. For example, the work by Chapman (Ref. 52) on the effects of sting-supports on base pressure shows that the separation pressure coefficient is alway negative, even for large stings. The cavity flow measurements such as in Figures 29 and 34 show negative pressure coefficients at separation. Data from Reference 6 for a geometry similar to that in Figure 35 but in a low subsonic freestream also indicate that the sting pressure coefficient immediately downstream of the disk is negative. Perhaps compressibility has enhanced the upstream effect of the relatively large diameter missile body. Evidence for this is given in Figure 36 where the pressure coefficient immediately downstream of the small disk (using the data of Figure 35) is plotted versus the freestream Mach number. The rapid increase in the value of C_p as M_∞ approaches one is quite apparent. A more complete explanation of this behavior must await further data and studies.

Returning to Figure 35, two reattachment points are evident with the value of the pressure coefficient being relatively large for the reattachment on the missile forebody. Mention has already been made (see Figure 18) that no reduction in drag was observed in the Trident nose spike studies for freestream Mach numbers less than one. Perhaps,

for the geometries considered in those studies (Refs. 2, 15 and 22) the reattachment is on a more forward facing portion of the missile nose and consequently the pressure is elevated above the value there without a spike. Conceivably a different spike geometry might move the reattachment further downstream on the missile nose and yield a drag reduction because of lower nose pressures. This is most likely what is happening in the investigations of Spooner (Ref. 27) where significant drag reductions were observed. It should also be noted that the Trident nose shape is quite rounded and has low drag and a high critical Mach number relative to the blunt Spooner body even without a probe or spike in front.

The strongly contrasting results of Spooner (Ref. 27) and the Trident studies (Refs. 2, 15 and 22) demonstrate that considerable care must be taken in using induced flow separation to reduce forebody drag. It is also clear that a substantial effort is necessary to obtain a thorough or even an engineering level of understanding of the phenomena involved.

F. Forward-facing steps

Chapman, et. al., in Reference 36 and Wu, et. al., in Reference 37, include extensive data concerning two-dimensional forward-facing steps in transonic and supersonic freestreams. Their data indicate that the flow typically separates about one step height ahead of the step for appoach boundary layers which are significantly thinner than the step height. Details of the separation process and separation distance are, in general, strong functions of the approaching boundary layer characteristics and freestream Mach number.

No data on axisymmetric forward-facing steps were found in the present investigation. When such information is available the data of Chapman (Ref. 36) and Wu (Ref. 37) will become extremely useful.

VI. Conclusion

As a method for reducing the drag of bodies in transonic freestreams an arrangement consisting of a plane-nosed circular cylinder axially aligned with the flow with a smaller diameter plane-nosed cylindrical probe coaxially extended ahead has been considered. Motivation for this configuration stems from several facts. A plane-nosed circular cylinder is a simple, volumetrically and structurally efficient shape and serves as a prototype for a wide variety of vehicles. Moreover, careful experiments have shown that for low subsonic and supersonic freestreams, the drag of a plane-nosed circular cylinder with the proper probe or frontbody placed in front can be made arbitrarily low. Some evidence exists which indicates that this is also true for transonic flows. The present investigation has been conducted to explore flow past probe/cylinder geometries and the possibilities of using a probe to reduce the drag of blunt-nosed axisymmetric bodies in transonic freestreams.

The emphasis of this study has been to obtain a description of the flow field which occurs for probe/cylinder combinations in transonic flow. If such a description is formulated, the likelihood of drag reductions and the geometrical arrangements for minimum drag can be more completely assessed. There appears, however, to be essentially no data available on the flow field surrounding probe/cylinder configurations in transonic freestreams. It is therefore necessary to attempt to construct the flow field from knowledge of related problems.

The flow past a probe/cylinder arrangement can be regarded as a problem of the interaction of separated flow from the probe face with

the separation which develops ahead of the step formed by the probe/cylinder junction. It is postulated that when these two separated regions merge the drag would then be a minimum. Thus a study of flow past plane-nosed cylinders and axisymmetric forward-facing steps should provide guidelines as to the behavior of probe/cylinder geometries. Data for transonic flow past axisymmetric forward-facing steps are also essentially non-existent. Some data do exist for plane-nosed cylinders and for related flows past cavities, rearward-facing steps and bases. These flows have been studied for insight they might provide into the probe/cylinder problem. The phenomenon of cavity opening is particularly relevant here.

A simple, semi-empirical free streamline analysis has been made to predict the geometries and free streamline pressure for the postulated low drag probe/cylinder flow. This flow is assumed to be one in which the flow separates from the probe face, forms a free streamline (actually a free shear layer) which then reattaches smoothly or tangentially to the sides of the cylinder. The trends predicted for the pressure coefficient are in qualitative agreement with what is suggested by certain experiments. The trends for the geometry are opposite of inferences from experiment.

From consideration of the various related flows a few especially important results should be noted.

1. For freestream Mach numbers greater than about 0.8, the flow at the outer edge of a plane-nosed cylinder is sonic and the separation pressure coefficient is nominally -0.4.

2. The length of the separated zone downstream of the face of a

plane-nosed cylinder varies from roughly $1\frac{1}{2}$ diameters at $M_\infty = 0$ to a maximum of 5 diameters at $M_\infty = 1$ and then decreases for supersonic freestreams.

3. The drag coefficient for the face of a plane-nosed cylinder is nicely approximated by $C_D = C_{p_o} + 0.2$ where C_{p_o} is the freestream stagnation pressure coefficient, for M_∞ between zero and nearly 3.

4. For cavity flows where the initial separation is parallel to the freestream the critical length to depth ratio for cavity opening is between 10 and 12 roughly independent of Mach number and geometry (i.e. two-dimensional, axisymmetric, three-dimensional).

5. For parallel separation cavity flows there appear to be several possible criteria for cavity opening (as viewed when keeping the cavity depth fixed and reducing the length from an initially large value). These are:

   a. equality of the reattachment and separation pressures,
   b. pressure coefficient at the base of the rearward-facing step going from a negative value to nominally zero,
   c. pressure coefficient at the base of the forward-facing step going from a positive value to nominally zero.

6. There is significant disagreement concerning the possibility of drag reduction at transonic speeds using probe induced separation among the very few available data sets. However, the available data are too limited, especially from those experiments which observed no drag reductions, for any real assessment of the situation to be made.

With regard to the present goal of using probe induced separation to reduce transonic blunt forebody drag there is a need for a series of thorough experiments to be performed. In a larger sense these experiments would provide insight into the more general subject of transonic separated flows. Studies of axisymmetric forward-facing steps are most needed, however axisymmetric rearward-facing steps and axisymmetric cavities are also deserving of significant attention. There appears to be very incomplete information available on these fundamental flows and our understanding of them is quite meager. Without a solid data base, situations involving these flows, such as the probe/cylinder problem, cannot be properly analyzed nor used in designs. Thus the possibilities for drag reduction using probe induced separation remain still very much unknown, and a description of the flow as a merging of several separation regions remains a qualitative model.

Item	Two-dimensional	Axisymmetric
reference length	h = ½ plate thickness	d = cylinder diameter
reattachment length	$\ell/2h = 4.5$	$\ell/d = 1.7$
separation bubble maximum height and location	$y_{max}/2h = 0.6$ at $x/2h = 1.9$	$y_{max}/d = 0.25$ at $x/d = 0.8$
separation bubble pressure coefficient	$C_p = -0.72$	$C_p = -0.65$

Table 1 Properties of Blunt Forebody Incompressible Separation Bubbles (from References 8 and 48)

Author	Geometry	M	Re	length/depth	cavity flow	boundary layer thickness/depth
Charwat	two dimensional	0.60	?	4 to 16; length varied	turbulent	0.45
Charwat	two dimensional	2.78	$1.5*10^6$ based on equivalent flat plate length; $2.94*10^5$/in	2.5 to 12; length varied	turbulent	0.5
Johannesen	axisymmetric	1.965	$3.4*10^5$ based on upstream flat plate length; $3.4*10^5$/in	1.6 to 16; length and depth varied	transition just downstream of initial separation	?
Rossiter	three dimensional	0.4 to 1.2	$1.1*10^5$ based on δ at initial separation; $1.8*10^5$/in	1 to 10; depth varied	turbulent	0.075 to 0.75, $\delta/L = 0.075$, $\delta^*/L = 0.013$
Wu	two dimensional	0.5 to 0.9	$1.43*10^7$ to $8.57*10^7$ based on upstream flat plate length; $4.2*10^5$/in to $2.5*10^6$/in	11 to 40 length varied	turbulent	?

Table 2 Cavity Flow Experimental Details

References

[1] Saunders, W. S., "Apparatus for Reducing Linear and Lateral Wind Resistance in a Tractor-Trailer Combination Vehicle," U. S. Patent No. 3,241,876, 1966.

[2] French, N. J. and Jecmen, D. M., "Transonic/Supersonic Wind Tunnel Investigation of Effects of Parametric Variations in Nose Fairing and Aerospike Geometry on Trident 1 C4 Missile Body Static Stability and Drag," Lockheed Missiles and Space Co., Sunnyvale, CA, LMSC-D 366908, September 1974.

[3] Polhamus, E. C., "Effect of Nose Shape on Subsonic Aerodynamic Characteristics of a Body of Revolution Having a Fineness Ratio of 10.94," NACA RM L57F25, August 1957.

[4] Norris, J. D. and McGhee, R. J., Effects of Bluntness on the Subsonic Drag of an Elliptical Forebody," NASA TN D-3388, April 1966.

[5] Rogers, R. M. and Butler, C. B., "Aerodynamics Characteristics of Several Bluff Body Configurations at Subsonic and Transonic Mach Numbers," AFATL-TR-72-25, February 1972.

[6] Koenig, K., "Interference Effects on the Drag of Bluff Bodies in Tandem," Ph.D. Thesis, California Institute of Technology, University Microfilms, 1978.

[7] Stanbrook, A., "A Correlation of the Forebody Drag of Cylinders with Plane and Hemispherical Noses at Mach Numbers from Zero to 2.5," ARC CP 709, 1964.

[8] Ota, T., "An Axisymmetric Separated and Reattached Flow on a Longitudinal Blunt Circular Cylinder," Journal of Applied Mechanics, June 1975, pp. 311-315.

[9] Roshko, A. and Koenig, K., "Interaction Effects on the Drag of Bluff Bodies in Tandem," in Aerodynamic Drag Mechanisms of Bluff Bodies and Road Vehicles, Sovran, G., Morel, T. and Mason, W. T., editors, Plenum, New York, 1978.

[10] Moeckel, W. E., "Flow Separation Ahead of Blunt Bodies at Supersonic Speeds," NACA TN 2415, 1951.

[11] Mair,W. A., "Experiments on Separation of Boundary Layers on Probes in Front of Blunt-Nosed Bodies in a Supersonic Air Stream," Phil. Mag., Ser. 7, Vol. 43, No. 342, July 1952, pp. 695-716.

[12] Beastall, D. and Turner, J., "The Effect of a Spike Protruding in Front of a Bluff Body at Supersonic Speeds," ARC R&M No. 3007, 1957.

[13] Crawford, D. H., "Investigation of the Flow Over a Spiked-Nose Hemisphere-Cylinder at a Mach Number of 6.8," NASA TN D-118, Dec. 1959.

[14] Stalder, J. R. and Nielsen, H. V., "Heat Transfer from a Hemisphere-Cylinder Equipped with Flow-Separation Spikes," NACA TN 3287, September 1954.

[15] Guenther, R. A. and Reding, J. P., "Fluctuating Pressure Environment of a Drag Reduction Spike," AIAA Paper 77-90, January 1977.

[16] Flynn, H. and Kryopoulos, P., "Truck Aerodynamics," Transactions of SAE, Vol. 70, 1962, pp. 297-308.

[17] Buckley, F. T., Jr. and Sekscienski, W. S., "Comparisons of Effectiveness of Commercially Available Devices for the Reduction of Aerodynamic Drag on Tractor-Trailers," SAE 750704, 1975.

[18] Lissaman, P. B. S., "Development of Device to Reduce the Aerodynamic Resistance of Trucks," SAE 750702, 1975.

[19] Mason, W. T., Jr., "Wind Tunnel Development of the Drag-Foiler --a System for Reducing Tractor-Trailer Aerodynamic Drag," SAE 750705, 1975.

[20] Cooper, K. R., "Wind Tunnel Investigations of Eight Commercially Available Devices for the Reduction of Aerodynamic Drag on Trucks," Road and Transportation Assn. of Canada Natl. Conf. Proc., 1976.

[21] Mason, W. T., Jr. and Beebe, P. S., "The Drag Related Flow Field Characteristics of Trucks and Buses," General Motors Research Publ. No. 2257, 1977.

[22] Reding, J. P., Guenther, R. A. and White, L. R., "Unsteady Aerodynamic Consideration in the Design of a Drag-Reduction Spike," Journal of Spacecraft and Rockets, Vol. 14, No. 1, January 1977.

[23] Karpov, B. G. and Piddington, M. J., "Effect on Drag of Two Stable Flow Configurations Over the Nose Spike of the 90mm T316 Projectile," BRL TN 955, October 1954.

[24] Album, H. H., "Regarding the Utility of Spiked Blunt Bodies," Journal of Spacecraft, Vol. 5, No. 1, January 1968, pp. 112-114.

[25] McGhee, R. J. and Staylor, W. F., "Aerodyanmic Investigation of Sharp Cone-Cylinder Spikes on 120 degree Blunted Cones at Mach Numbers of 3.00, 4.50, and 6.00," NASA TN D-5201, June 1969.

[26] Walchner, O. and Sawyer, F. M., "Effect of Nose Spikes on the Stability of Finless and Spinless Blunt Bodies in Free Supersonic Flight," ARL TR 60-273, August 1960.

[27] Spooner, S. H., "Static Longitudinal Stability Characteristics of a Series of 90-Millimeter Artillery Shells at Mach Numbers of 0.8, 0.9, 1.0, and 1.2," NACA RM SL56D27, May 1956.

[28] Brennen, C., "A Numerical Solution of Axisymmetric Cavity Flows," Journal of Fluid Mechanics, Vol. 37, 1969, pp. 671-688.

[29] Strueck, H. G., "Discontinuous Flows and Free Streamline Solutions for Axisymmetric Bodies at Zero and Small Angles of Attack," NASA TN D-5634, 1970.

[30] Zorea, C. and Rom, J., "Effect of a Spike on the Drag and on the Aerodynamic Stability of Blunt Bodies in Supersonic Flow," Journal of Spacecraft, Vol. 7, No. 8, August 1970, pp. 1017-1019.

[31] Shang, J. S., Hankey, W. L. and Smith, R. E., "Flow Oscillations of Spike-Tipped Bodies," AIAA Journal, Vol. 20, No. 1, January 1982, pp. 25-26.

[32] Whitfield, D. L. and Thomas, J. L., "Transonic Viscous-Inviscid Interaction Using Euler and Inverse Boundary-Layer Equations," in Viscous Flow Computational Methods, W. T. Habashi, editor, Pineridge Press, Swanson U. K., 1983.

[33] Winchenbach, G. L. and Buff, R. S., "Memo for Record: Drag Data for a Generic Tactical Munitions Dispenser (TMD), "Aeroballistic Research Facility, Eglin AFB, FL August 8, 1983.

[34] Charwat, A. F., Roos, J. N., Dewey, F. C., Jr. and Hitz, J. A., "An Investigation of Separated Flows--Part I: The Pressure Field," Journal of the Aerospace Sciences, June 1961, pp. 459-470.

[35] Stanbrook, A., "Experimental Pressure Distributions on a Plane-nosed Cylinder at Subsonic and Transonic Speeds," ARC R&M No. 3425, 1966.

[36] Chapman, D. R., Kuehn, D. M. and Larson, H. K., "Investigation of Separated Flows in Supersonic and Subsonic Streams with Emphasis on the Effect of Transition," NACA TN 3869, March 1957.

[37] Wu, J. M., Chen, C. H., Moulden, T. H., Reddy, K. C., Collins, F. G., Nygaard, R., Kuwano, H., Vakili-Dast-Jerd, Ahmad and Sickles, W., "Fundamental Studies of Subsonic and Transonic Flow Separation: Part II--Second Phase Summary Report," AEDC-TR-77-103, December 1977.

[38] Rossiter, J. E., "Wind-Tunnel Experiments on the Flow Over Rectangular Cavities at Subsonic and Transonic Speeds," ARC R&M 3438, 1966.

[39] Johannsen, N. H., "Experiments on Supersonic Flow Past Bodies of Revlolution with Annular Gaps of Rectangular Section," Phil. Mag, Ser. 7, Vol. 46, No. 372, Jan. 1955, pp. 31-39.

[40] Roshko, A. and Thomke, G., "Observations of Turbulent Reattachment Behind an Axisymmetric Downstream-Facing Step in Supersonic Flow," AIAA Journal, Vol. 4, No. 6, June 1966, pp. 975-980.

[41] Merz, R. A., Przirembel, C. E. G. and Page, R. H., "Subsonic Axisymmetric Near-Wake Studies," AIAA Paper 77-135, January 1977.

[42] Ericsson, L. E. and Reding, J. P., "Review of Support Interference in Dynamic Tests," AIAA Journal, Vol. 21, No. 12, December 1983, pp. 1652-1666.

[43] Perkins, E. W., "Experimental Investigation of the Effects of Support Interference on the Drag of Bodies of Revolution at a Mach Number of 1.5," NACA TN 2292, February 1951.

[44] Kuechemann, D. and Weber, J., Aerodynamics of Propulsion, McGraw-Hill, New York, 1953.

[45] Schlichting, H. and Truckenbrodt, E., Aerodynamics of the Aeroplane, translation of Aerodynamik des Flugzeuges by H.J. Ramm, McGraw-Hill, New York, 1979.

[46] Arabshahi, A., "Correlations for the Drag Coefficients of Blunt Circular Cylinders in Transonic Axial Flow," M. S. Thesis, Mississippi State University, May 1984.

[47] Hoerner, S. F., Fluid-Dynamic Drag, Hoerner Fluid Dynamics, Brick Town, NJ, 1965.

[48] Ota, T. and Itasaka, M., "A Separated and Reattached Flow on a Blunt Flat Plate," Journal of Fluids Engineering, March 1976, pp. 79-86.

[49] Nicolai, L. M., Fundamentals of Aircraft Design, published by author, Aerospace Engineering, University of Dayton, Dayton, OH, 1975.

[50] Eaton, J.K. and Johnston, J. P., "A Review of Research on Subsonic Turbulent Flow Reattachment," AIAA Journal, Vol. 19, No. 9, September 1981, pp. 1093-1101.

[51] Chow, W. L. and Shih, T. S., "Transonic Flow Past a Backward-Facing Step," AIAA Journal, Vol. 15, 1977, pp. 1342-1343.

[52] Chapman, D. R., "An Analysis of Base Pressure at Supersonic Velocities and Comparison with Experiment," NACA TN 2137,July 1950.

[53] Roshko, A., "Some Measurements of Flow in a Rectangular Cutout," NACA TN 3488, August 1955.

[54] Gharib, M., "The Effect of Flow Oscillations on Cavity Drag, and a Technique for Their Control," Ph.D. Thesis, California Institute of Technology, University Microfilms, 1984.

[55] McGregor, O. W. and White, R. A., "Drag of Rectangular Cavities in Supersonic and Transonic Flow Including the Effects of Cavity Resonance," AIAA Journal, Vol. 8, 1970, pp. 1959-1964.

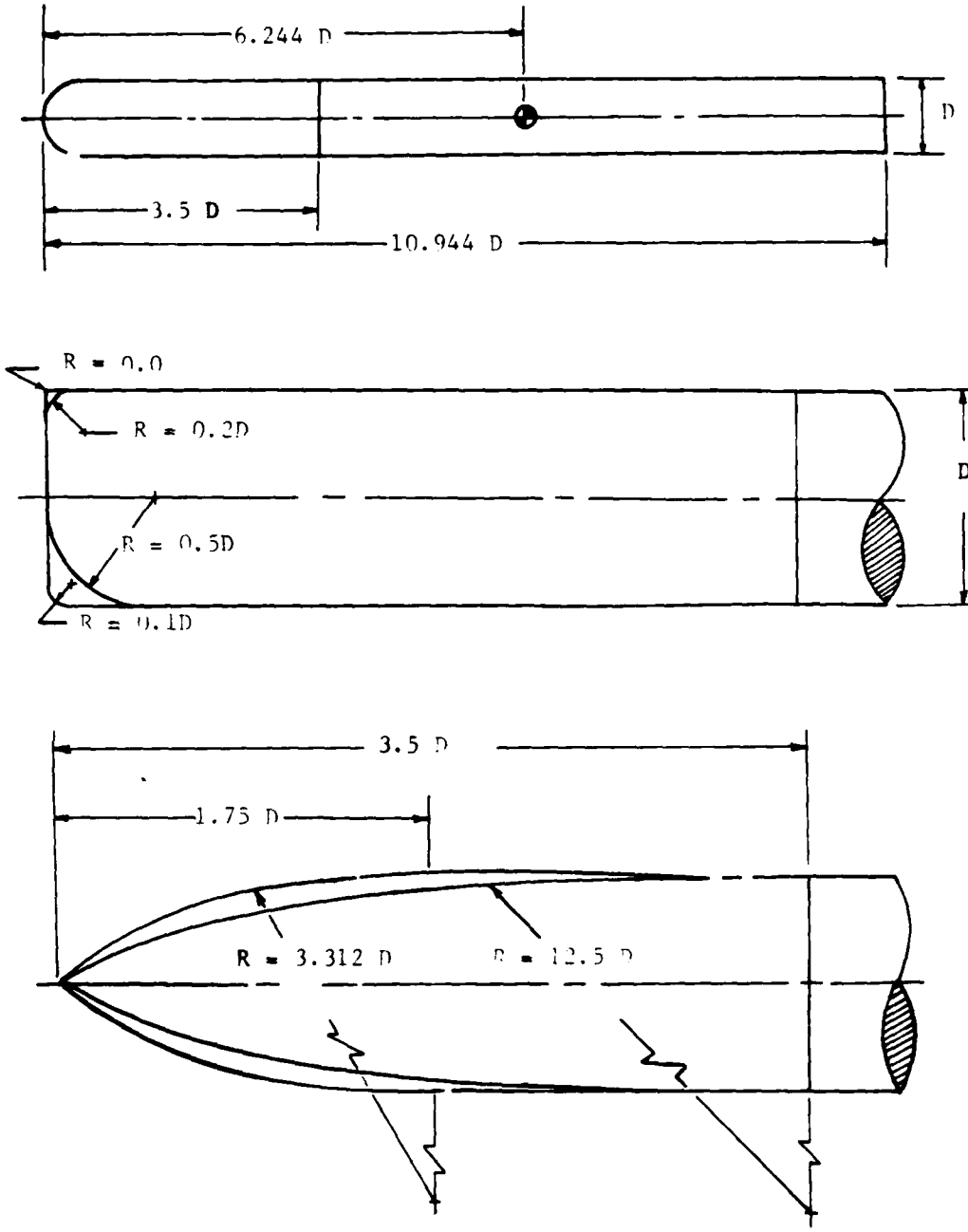

Figure 1 Circular Arc Forebodies (from Fig. 2, Ref. 3)

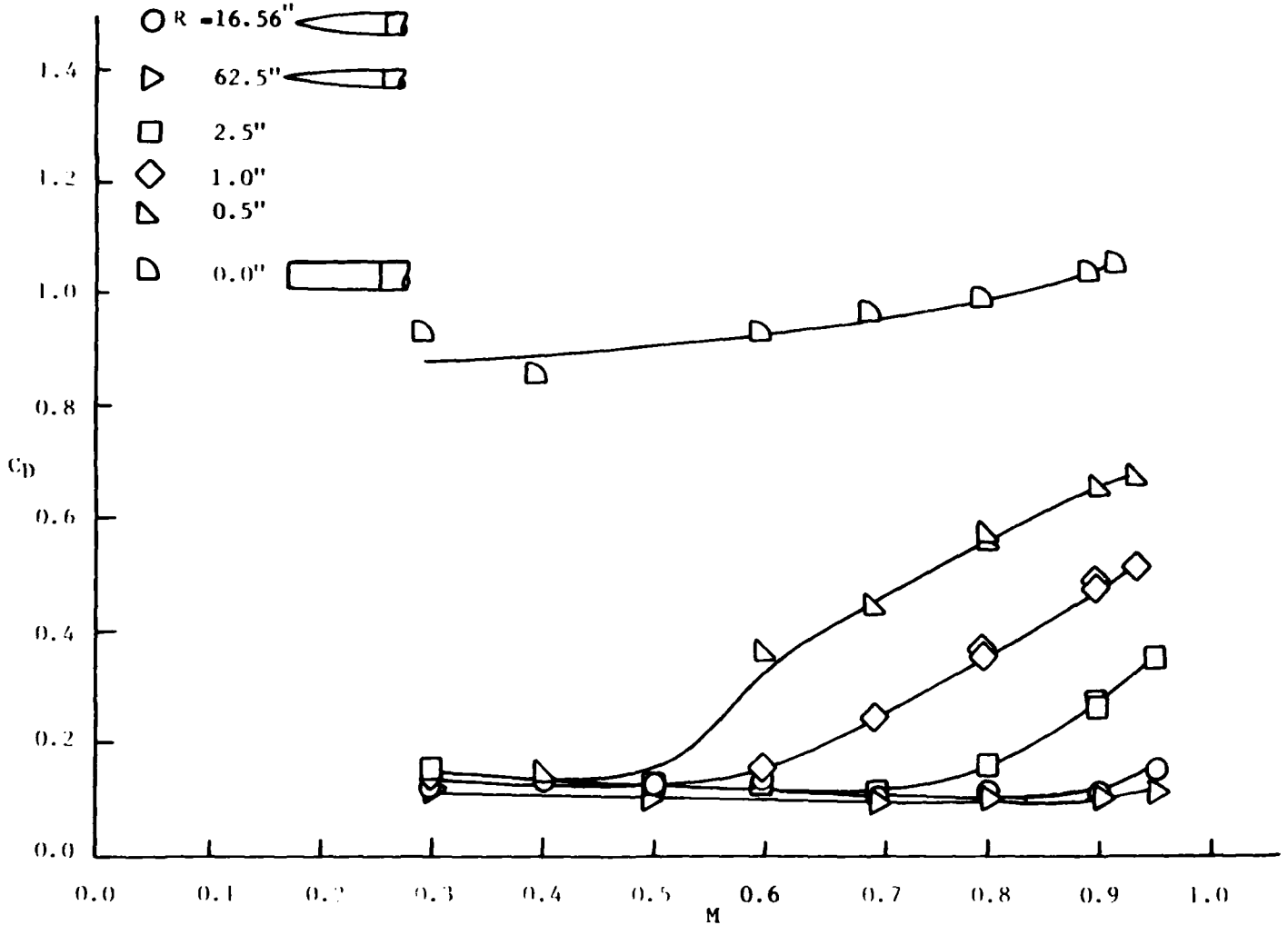

Figure 2 Drag Coefficients of Circular Arc Forebodies (from Fig. 7, Ref. 3)

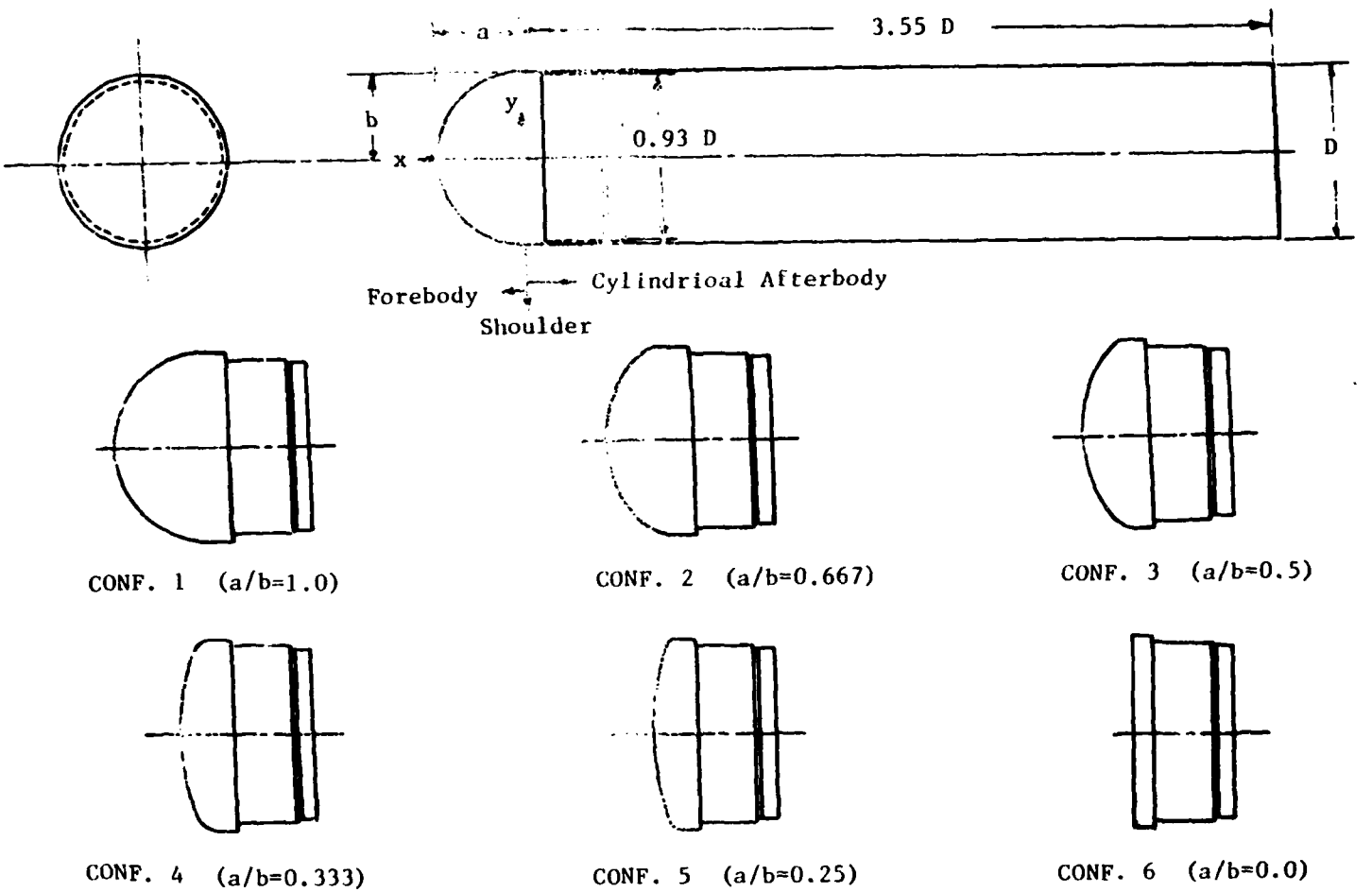

Figure 3 Elliptic Arc Forebodies (from Fig. 1, Ref. 4)

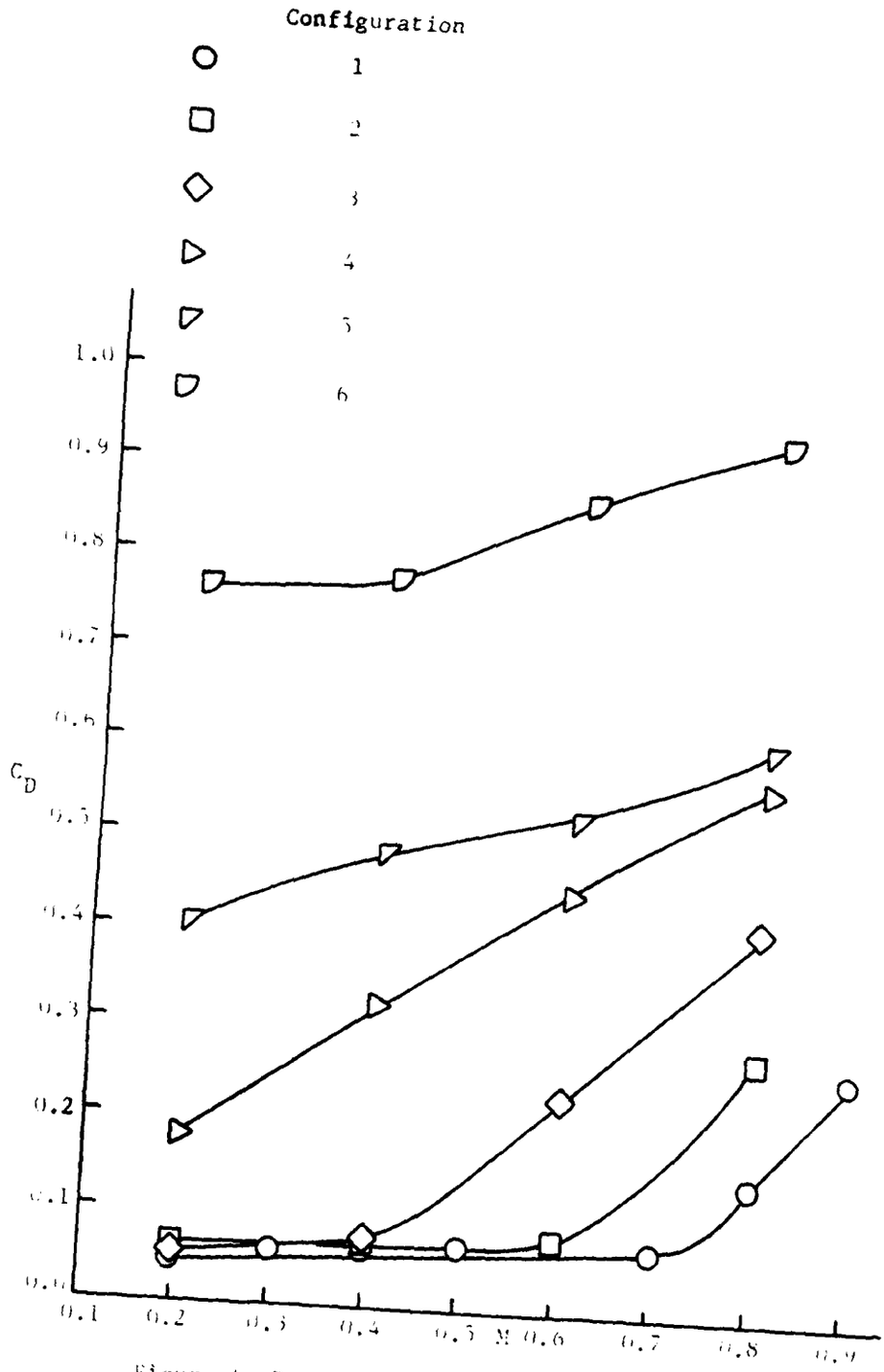

Figure 4 Drag Coefficients of Elliptical Arc Forebodies (from Fig. 7, Ref. 4)

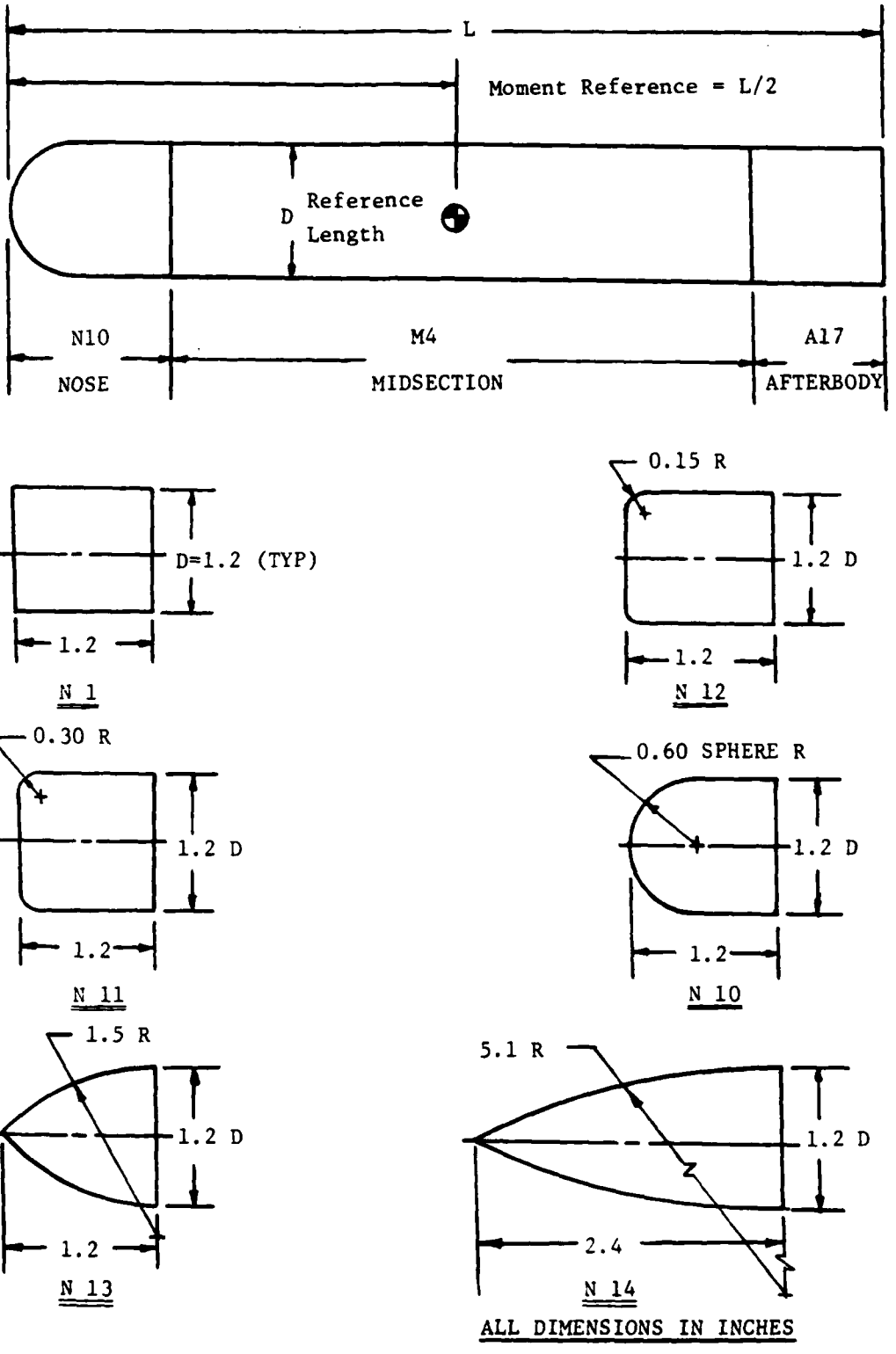

Figure 5 A Sequence of Blunt Projectiles (from Fig. 3, Ref. 5)

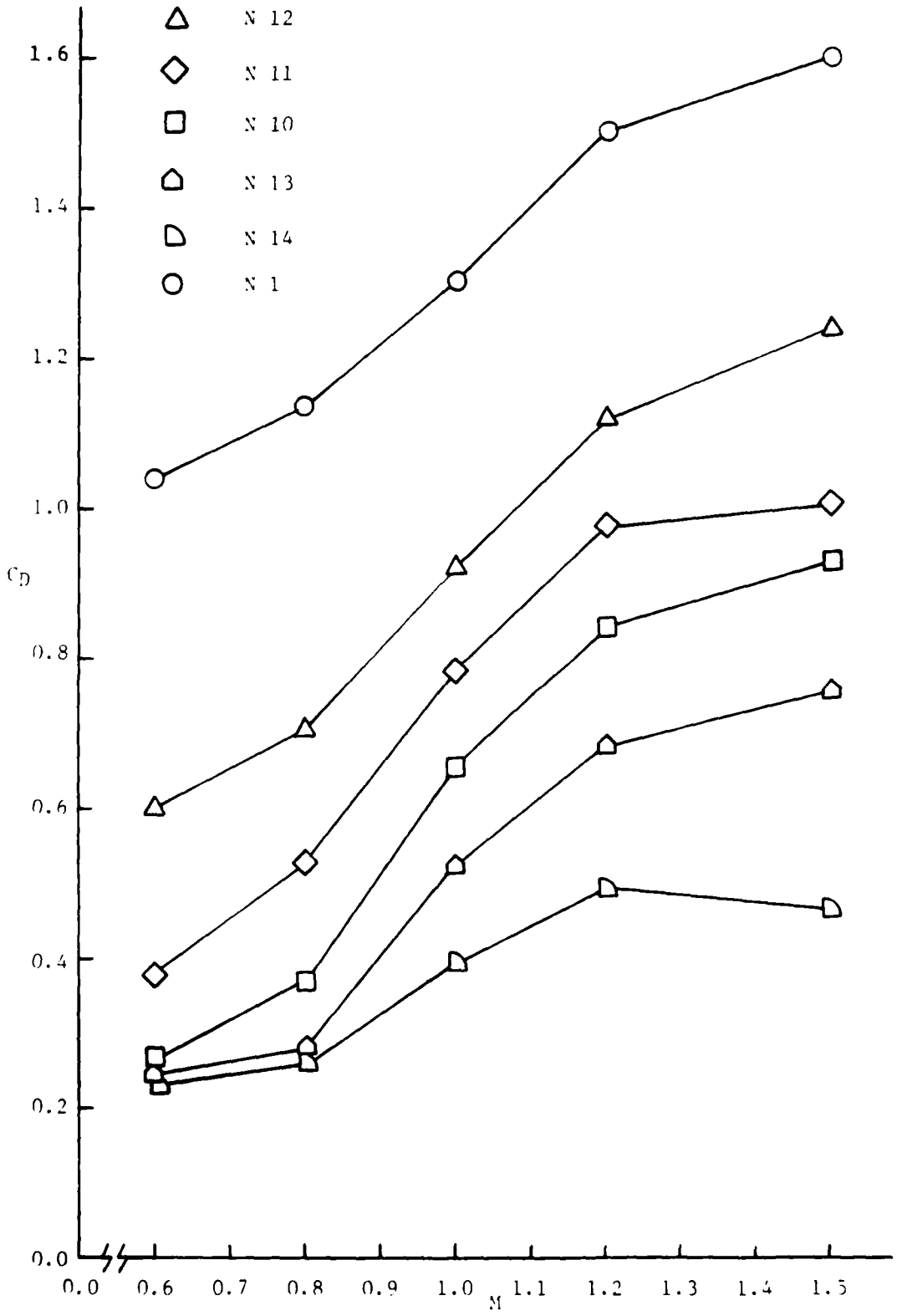

Figure 6 Drag Coefficients of a Sequence of Blunt Projectiles (from Ref. 5)

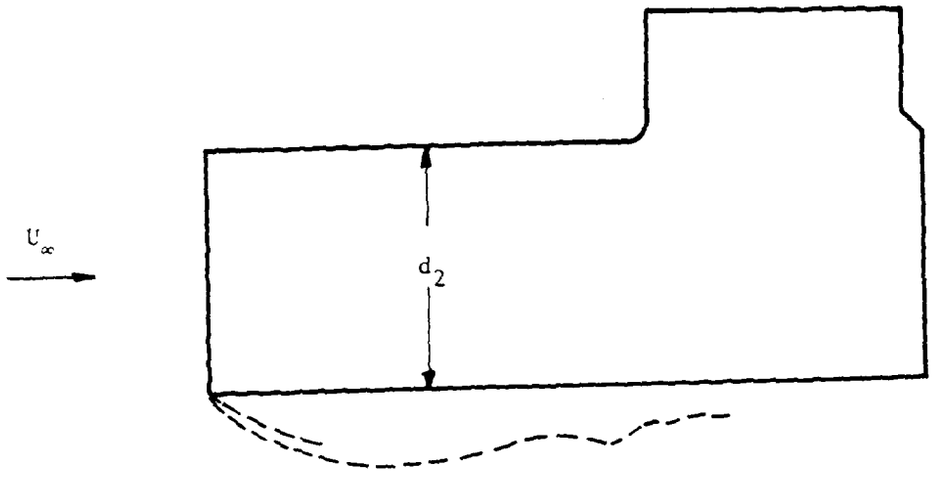

a) short time average

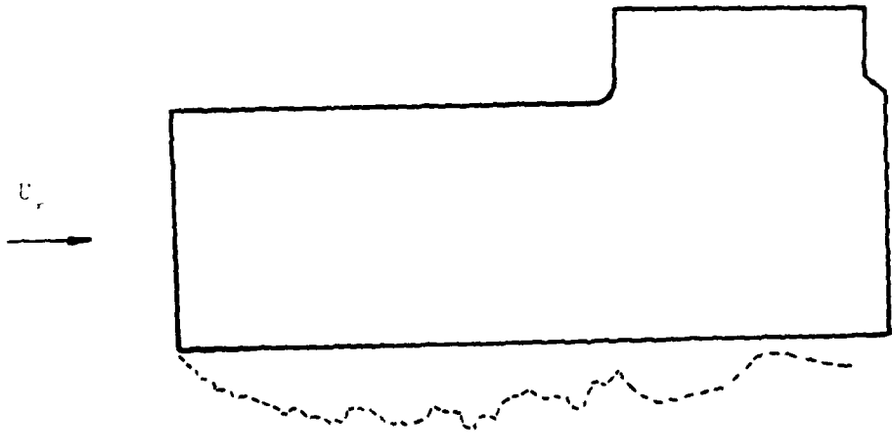

b) instantaneous

Figure 7 Incompressible Flow Past a Plane-Nosed Circular Cylinder. Boundary of Separated Zone (sketched from Fig. 5, Ref. 6).

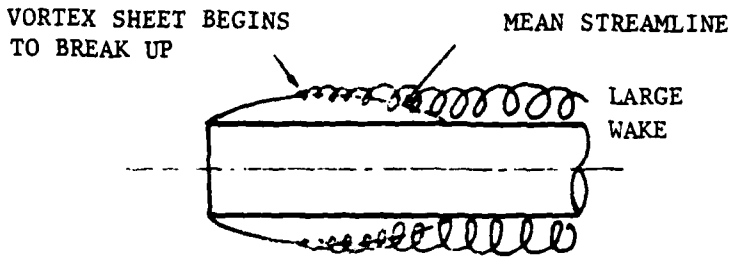

(a) SUBSONIC

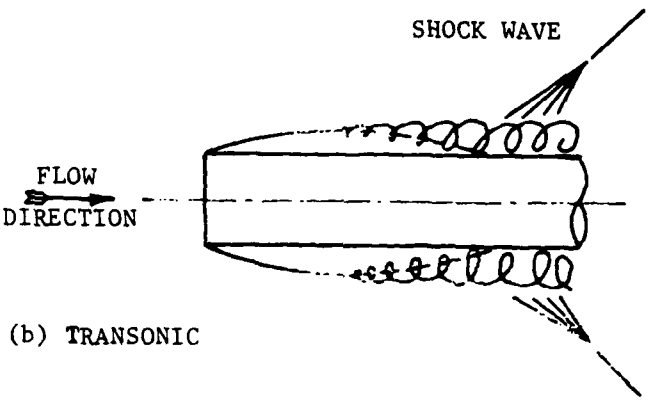

(b) TRANSONIC

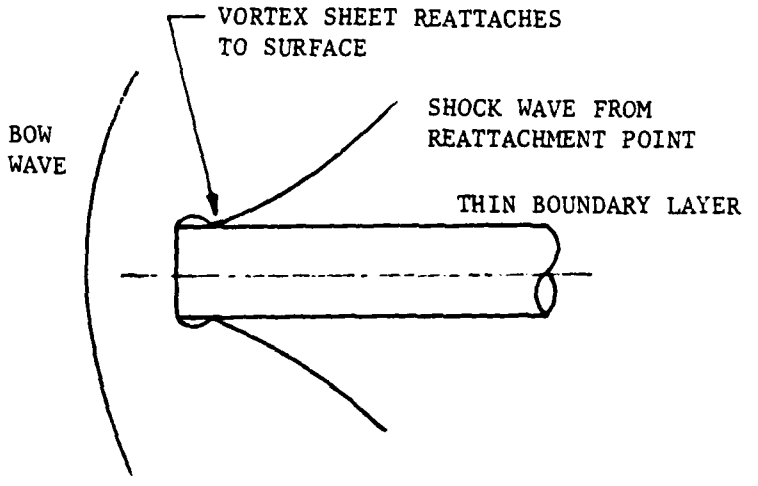

(c) SUPERSONIC

Figure 8 Transonic Flow Properties of a Typical Blunt Forebody (from Fig. 2, Ref. 35)

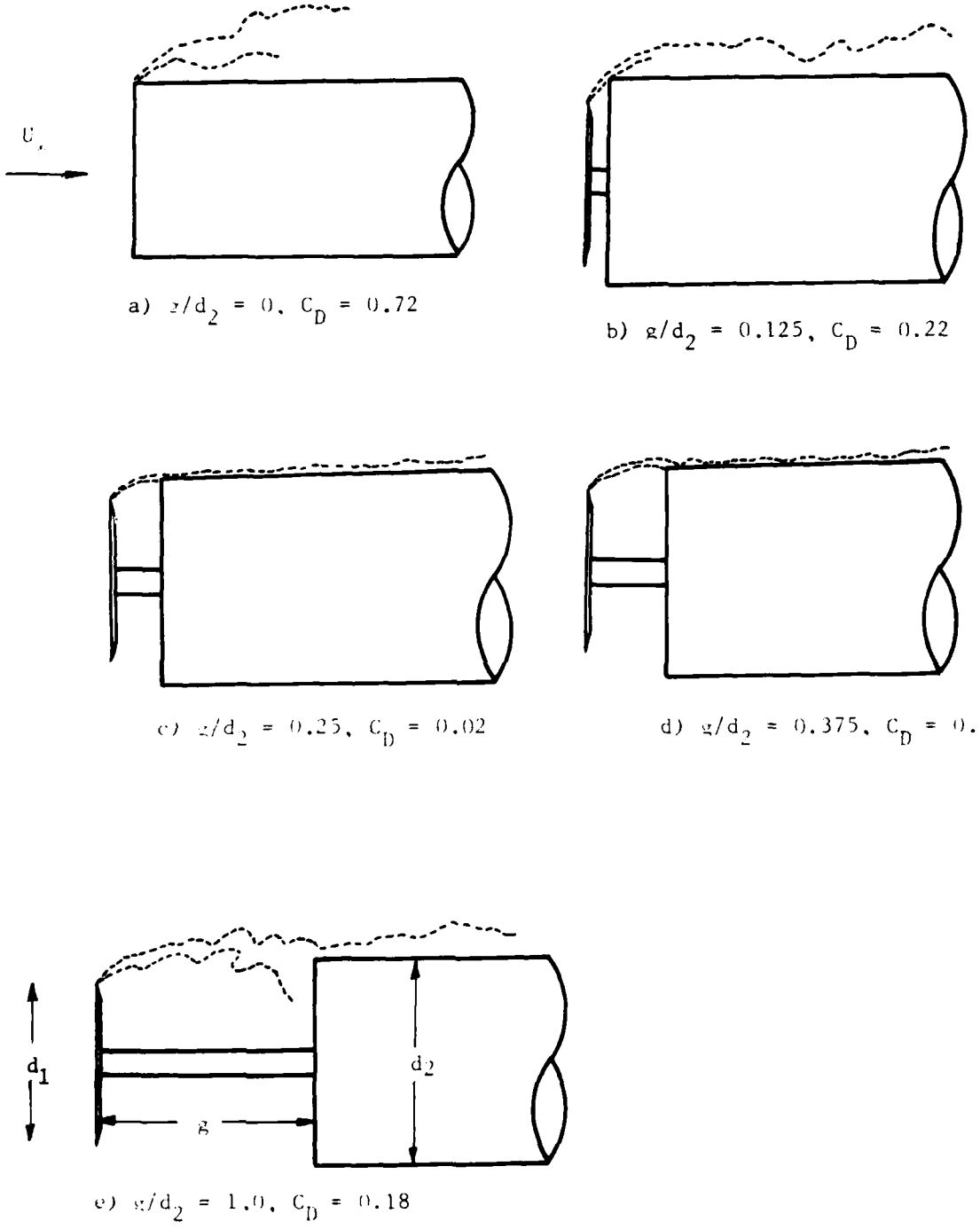

Figure 9 Incompressible Flow Past a Disk/Cylinder, $d_1/d_2 = 0.75$. Boundary of Free Shear Layer (sketched from Fig. 3, Ref. 9).

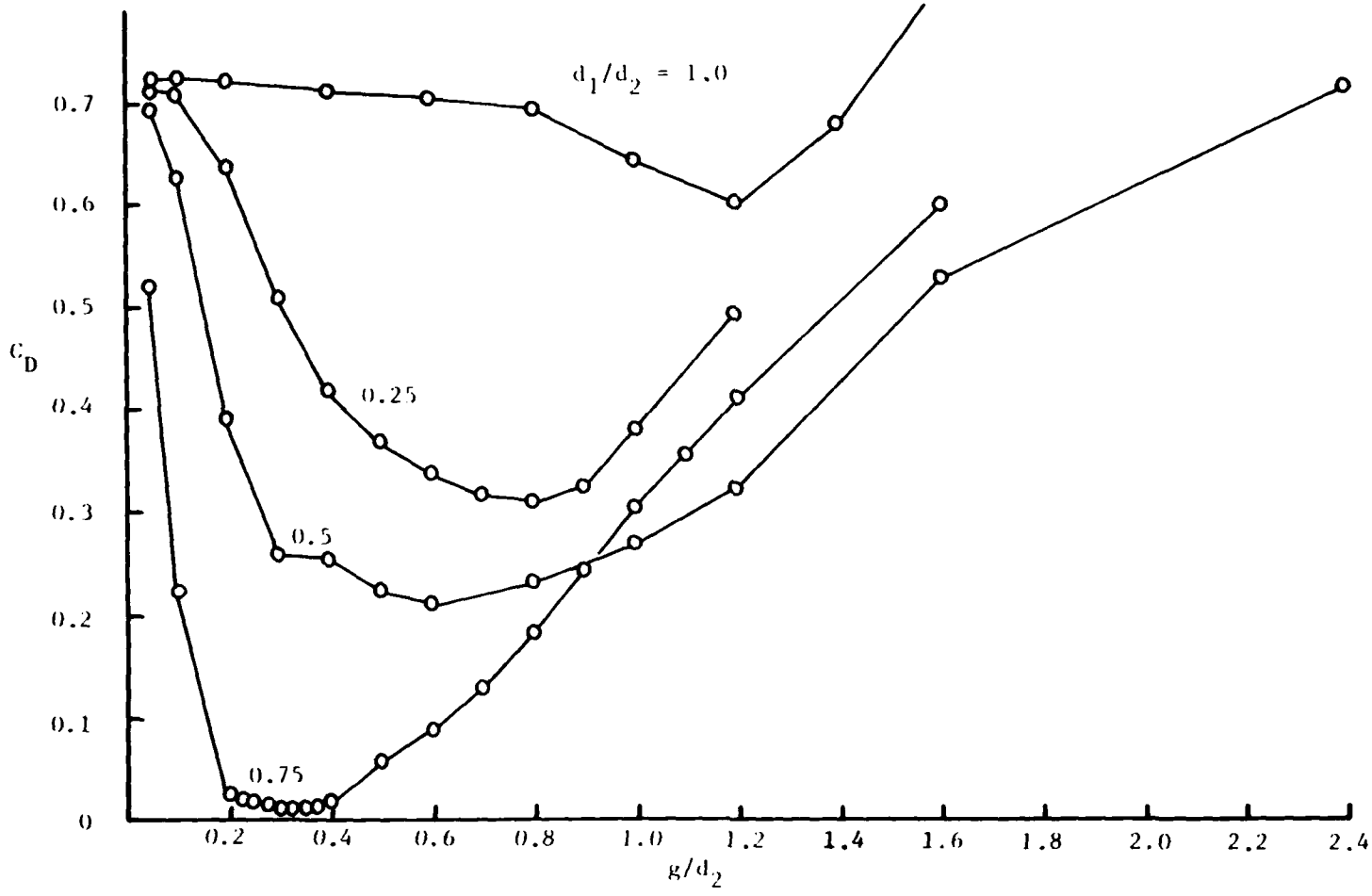

Figure 10 Forebody Drag Coefficient of Disk/Cylinder in Incompressible Flow, Coefficient Includes Force on Disk and Cylinder Face. (from Fig. 3, Ref. 6)

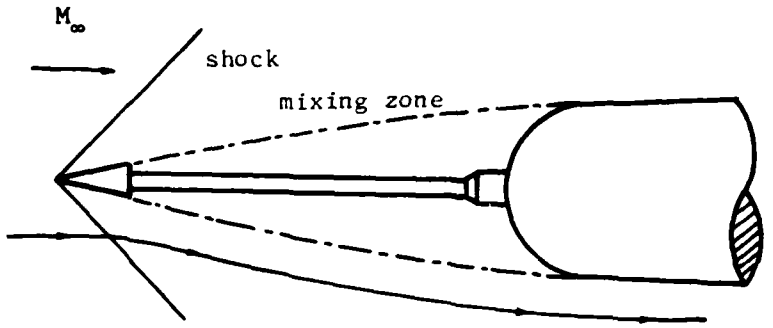

a) Conical Windshield

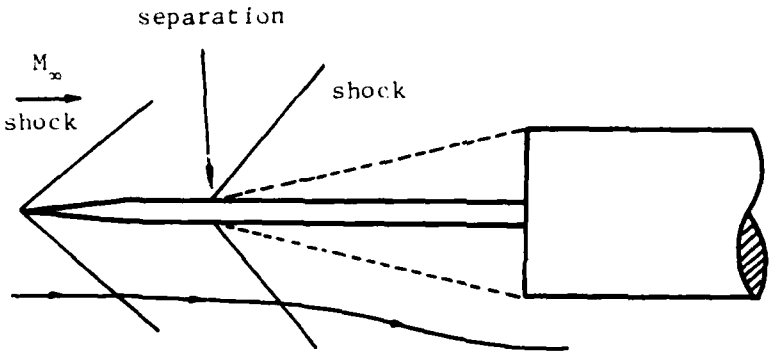

b) Spike

Figure 11 Supersonic Flow Past Bluff Cylinders with Drag Reduction Spikes (from Fig. 3, Ref. 12).

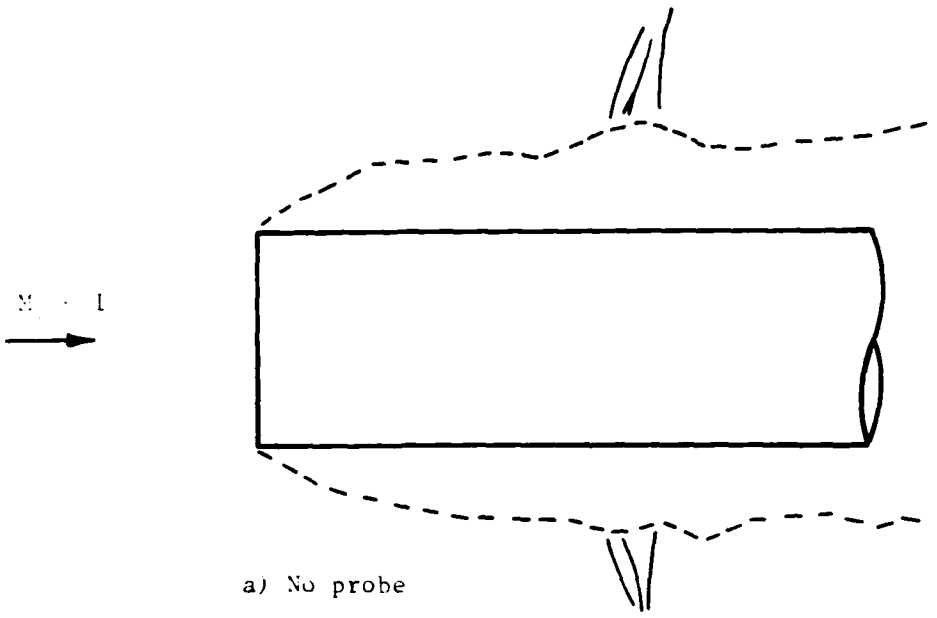

a) No probe

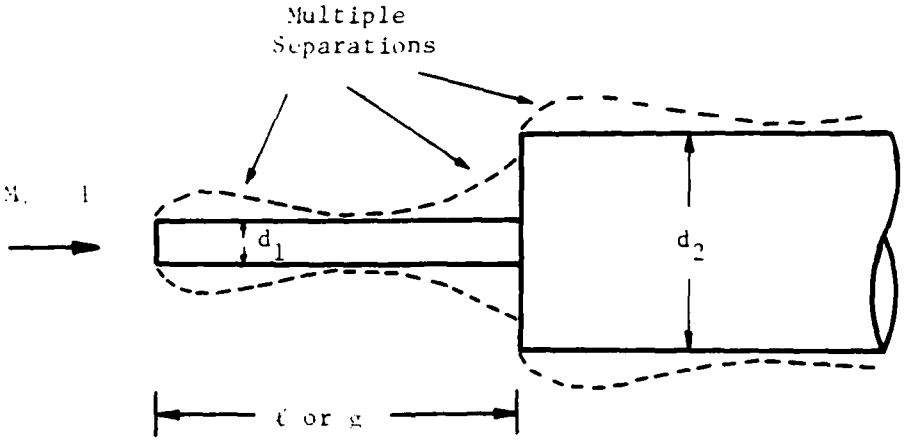

b) Long probe

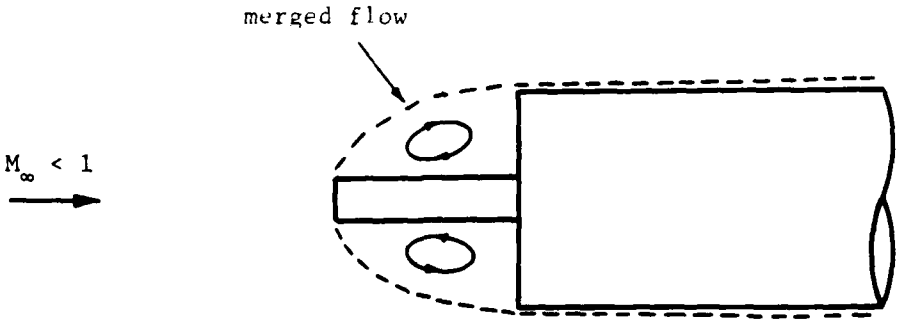

c) Optimum probe

Figure 12 Possible Flow Patterns for Probe/Cylinders in Subsonic Flow

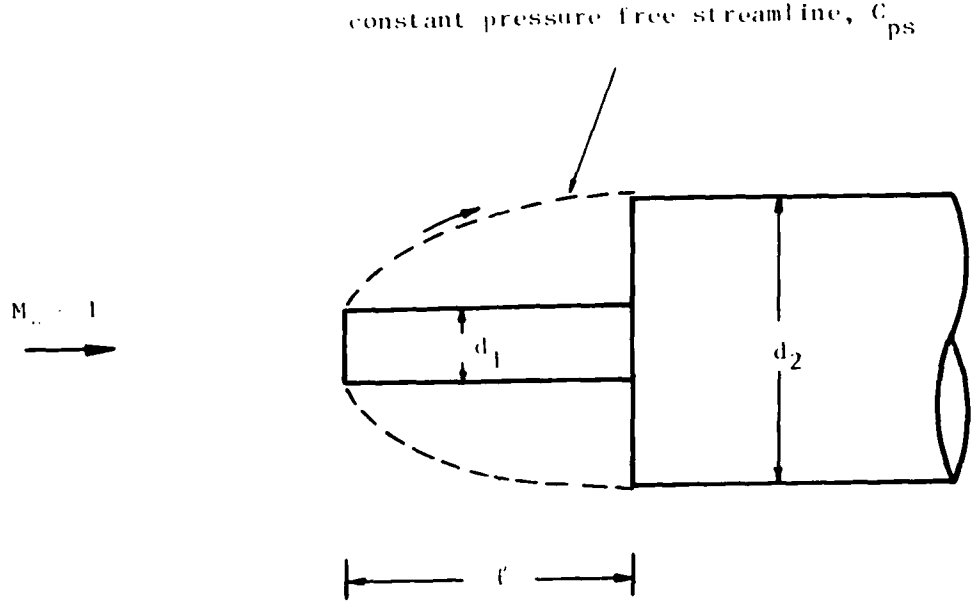

Figure 13 Flow Model for Free Streamline Analysis

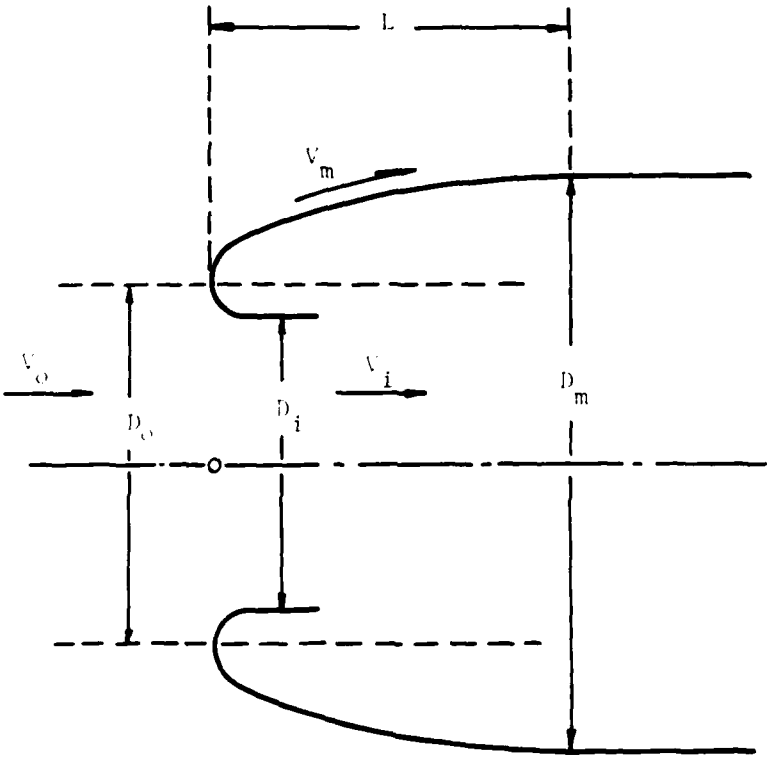

Figure 14 Geometry of Optimum Engine Air Intake (from Fig. 4-16, Ref. 44)

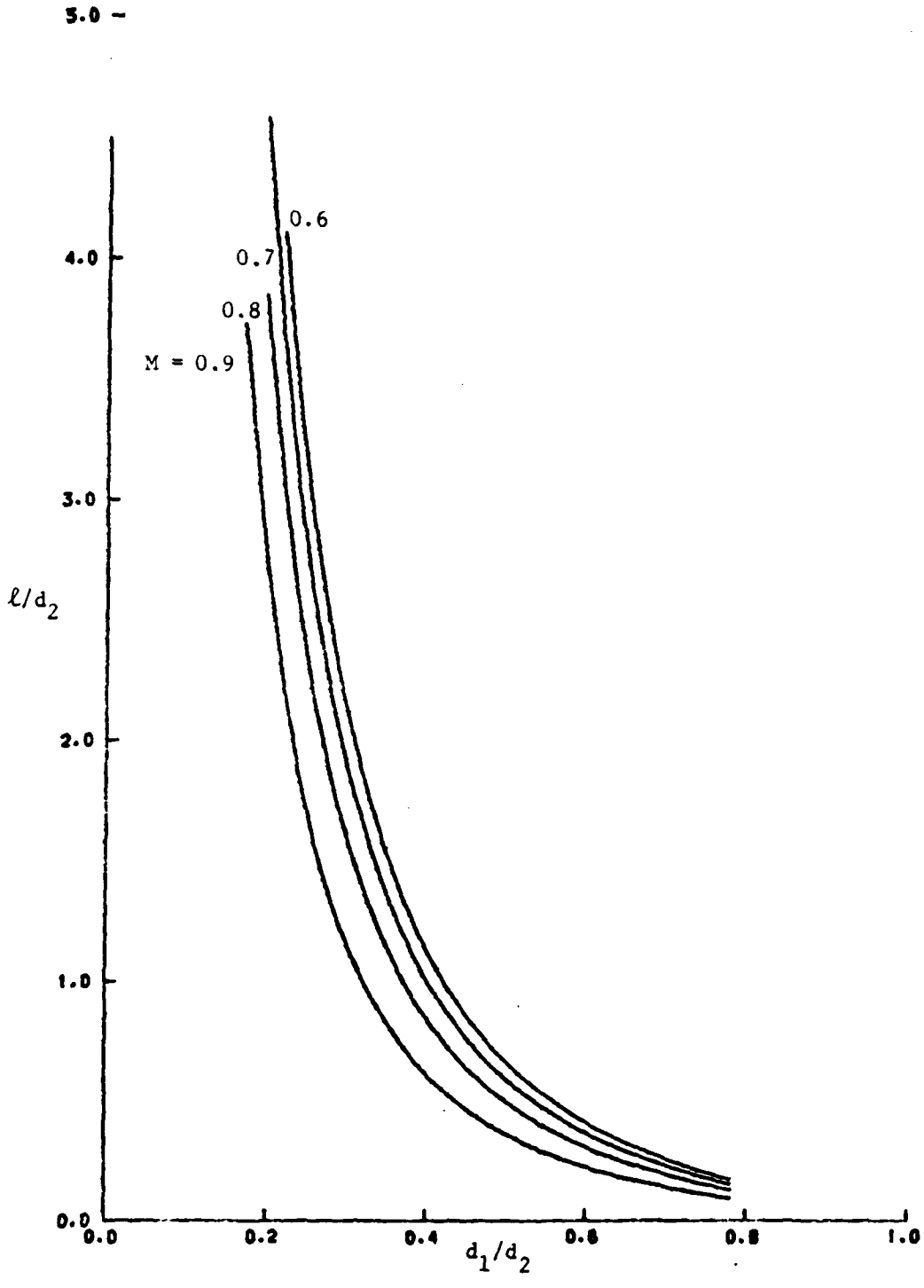

Figure 15a Predicted Probe/Cylinder Geometry from Free Streamline Analysis

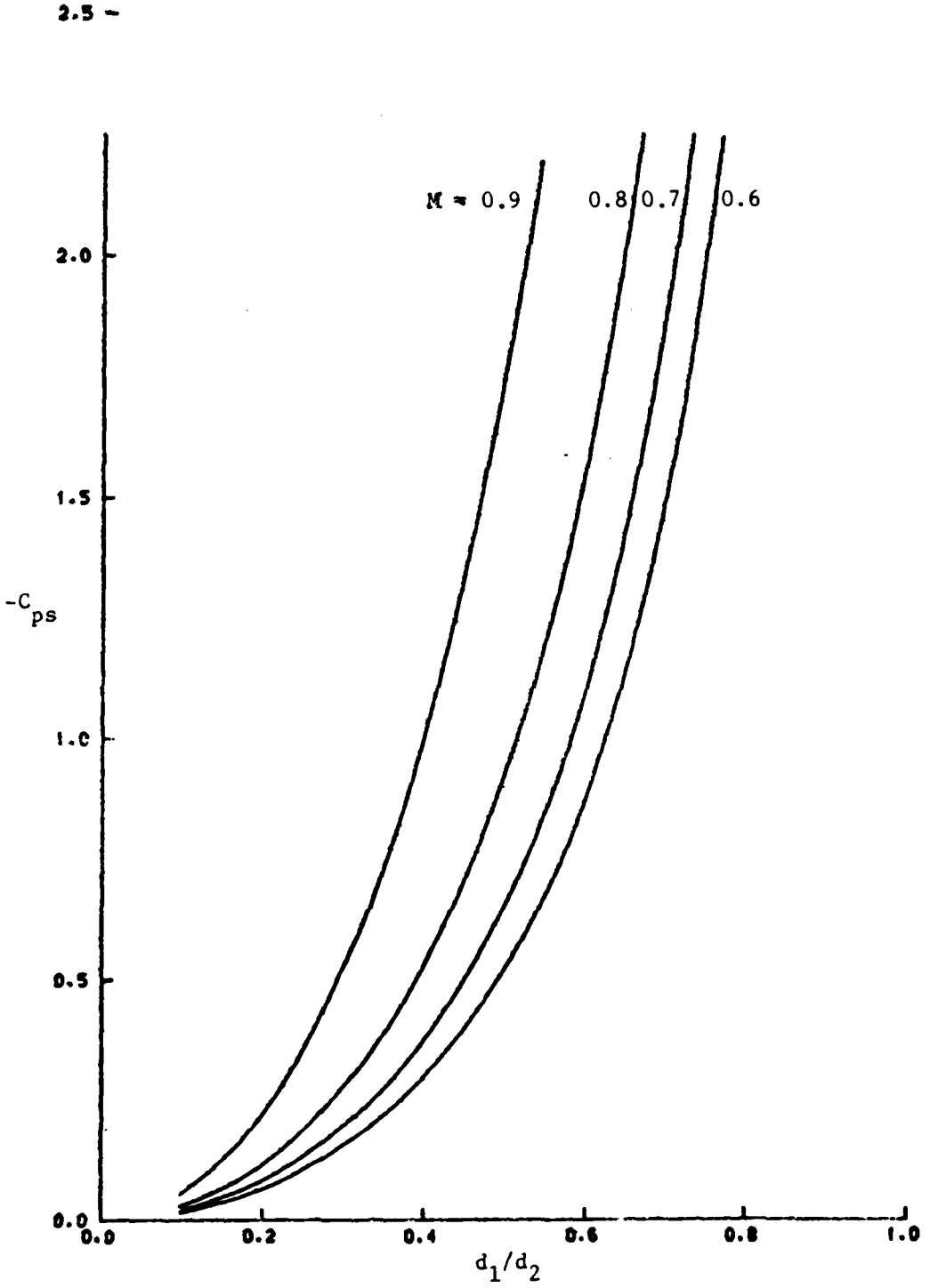

Figure 15b Predicted Free Streamline Pressure Coefficient from Free Streamline Analysis

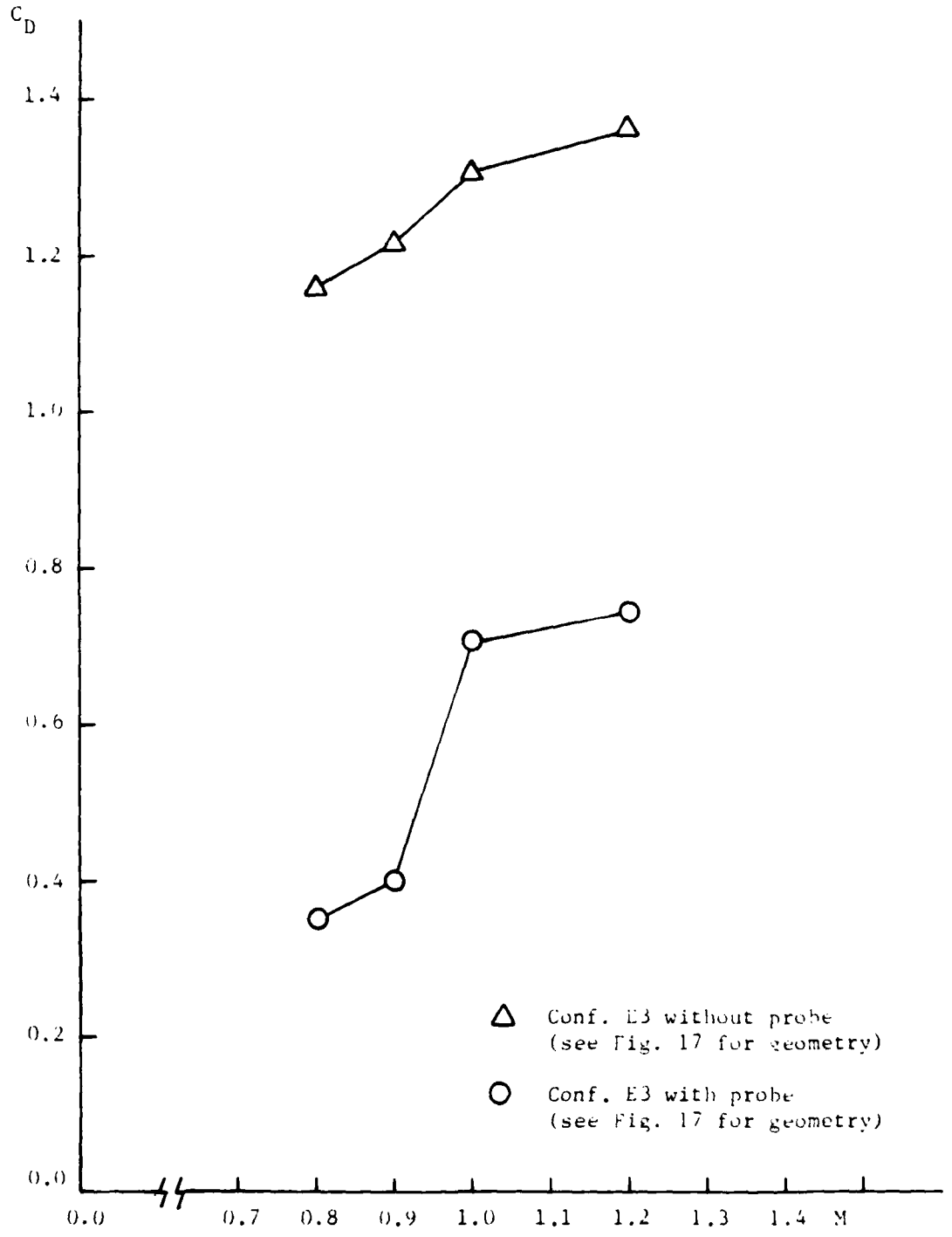

Figure 16 Drag Coefficients of a Blunt Projectile With and Without a Probe as a Function of Mach Number (from Fig. 16, Ref. 27)

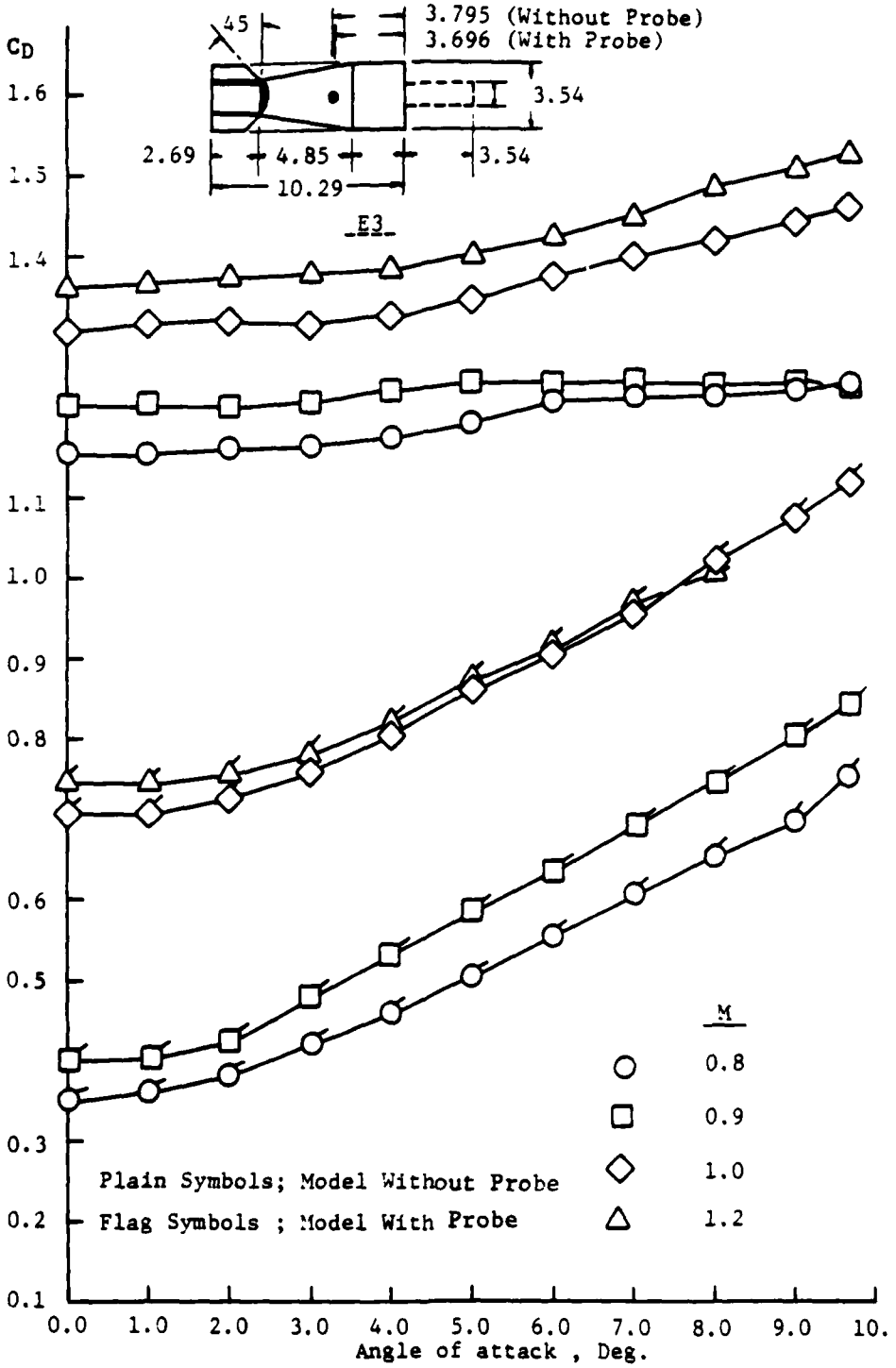

Figure 17 Drag Coefficients of a Blunt Projectile With and Without a Probe as a Function of Incidence Angle (from Fig. 16, Ref. 27)

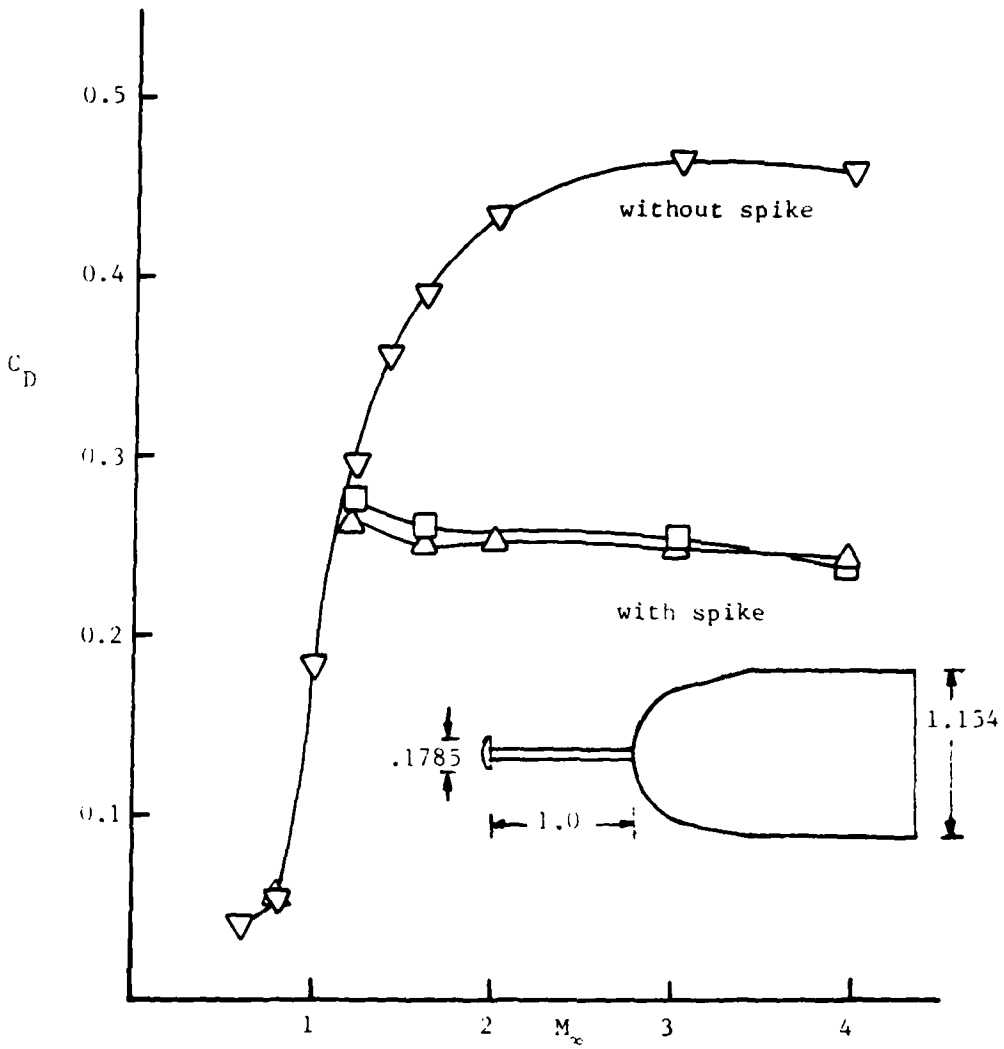

Figure 18 Effect of Aerospike on Forebody Drag Coefficient (from Fig. 19, Ref. 2)

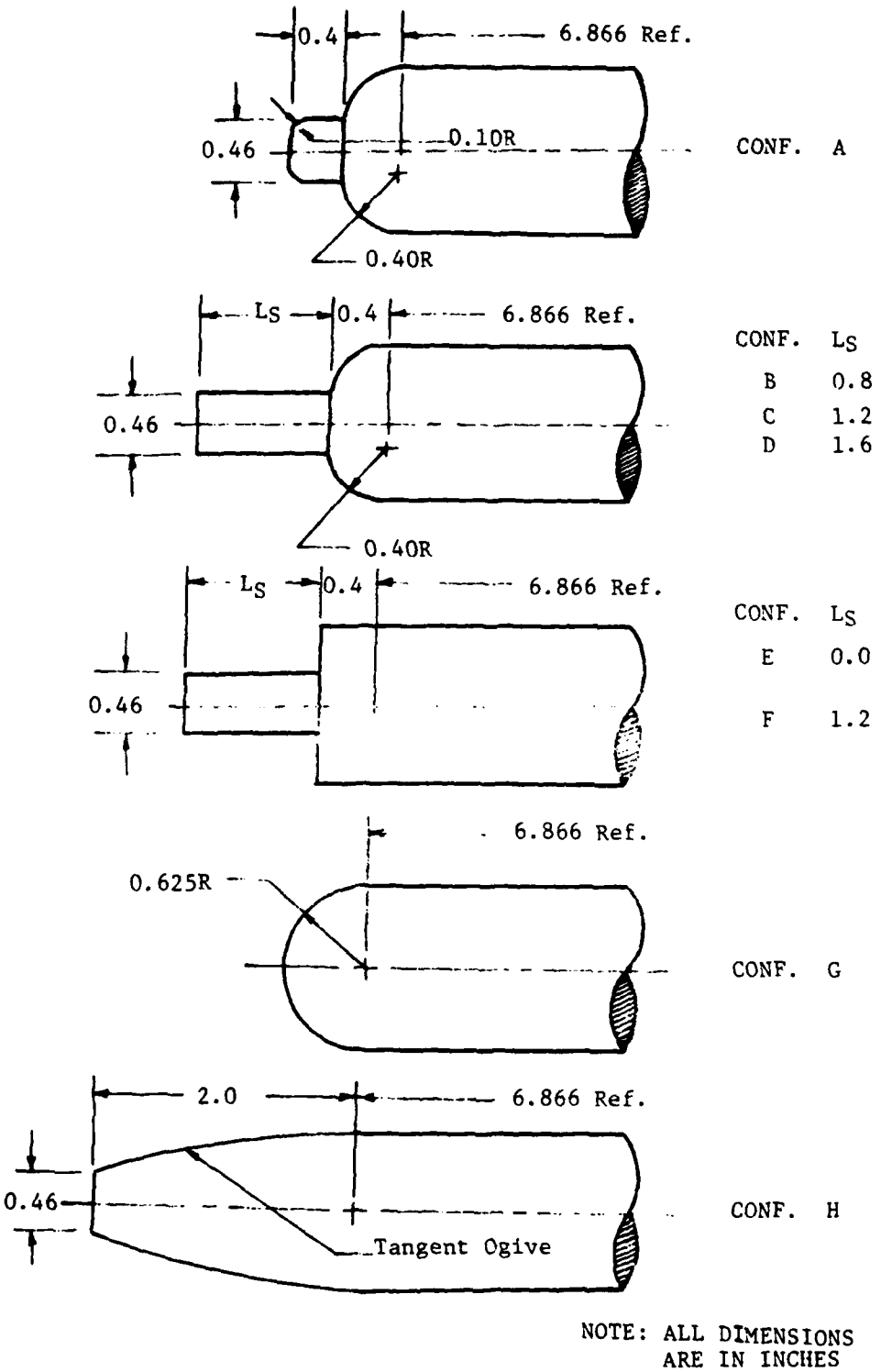

Figure 19a A Sequence of Blunt Projectiles (from Fig. 2, Ref. 33)

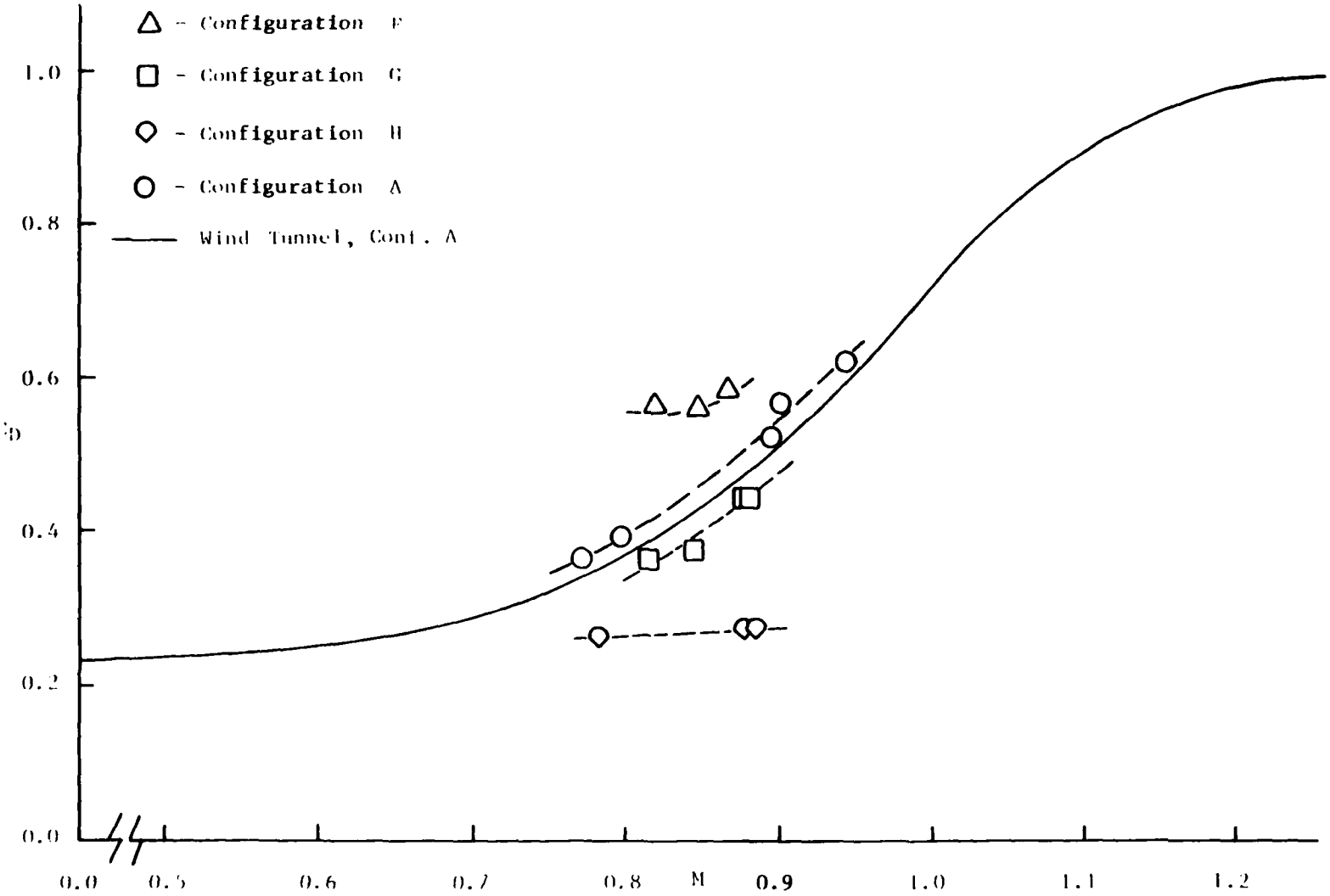

Figure 19b (from Fig. 4, 5, 6, Ref. 33)

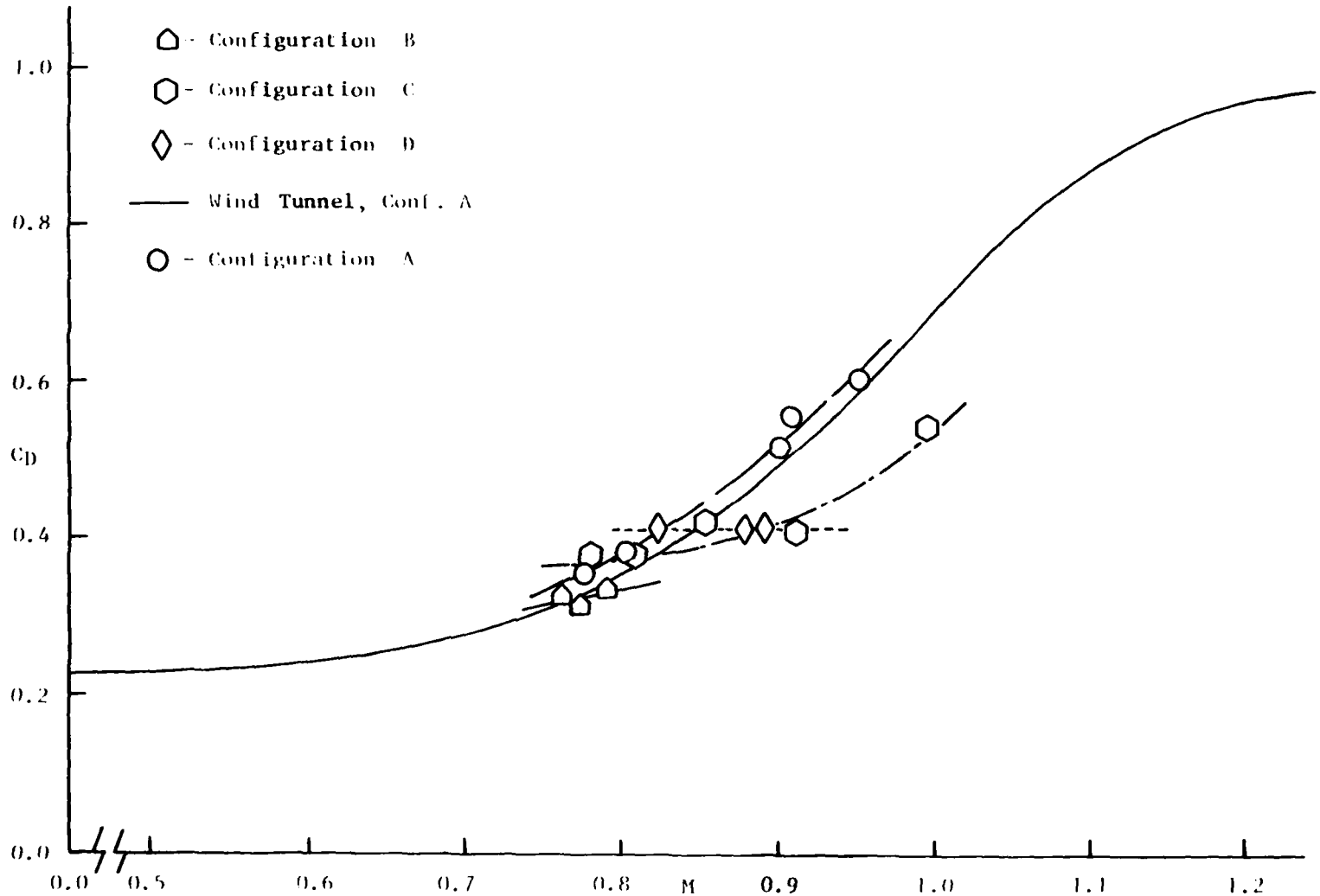

Figure 19c (from Fig. 4, 5, 6, Ref. 3)

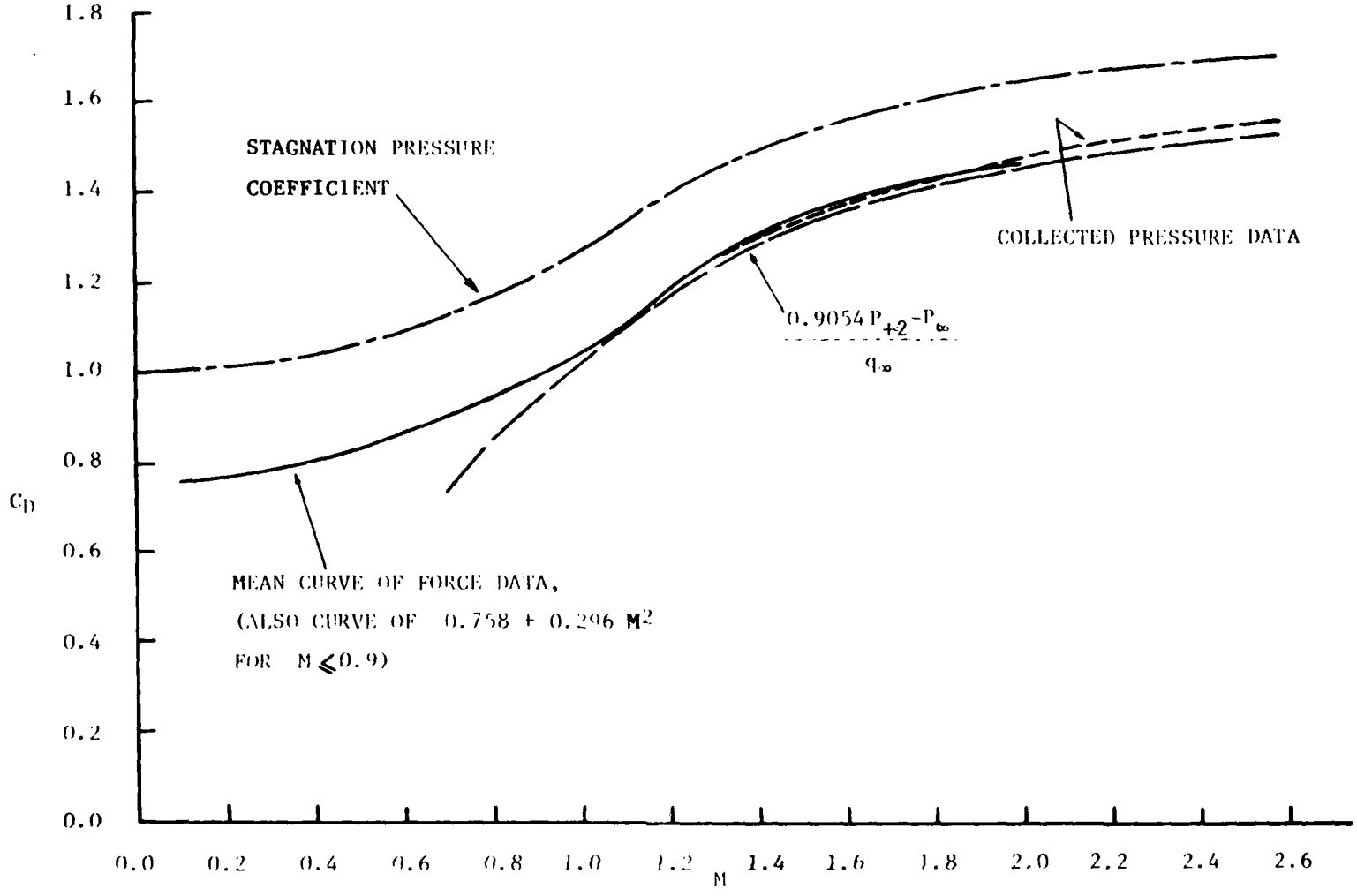

Figure 20 Drag Coefficients of Plane-Nosed Circular Cylinders
(from Fig. 3, Ref. 7)

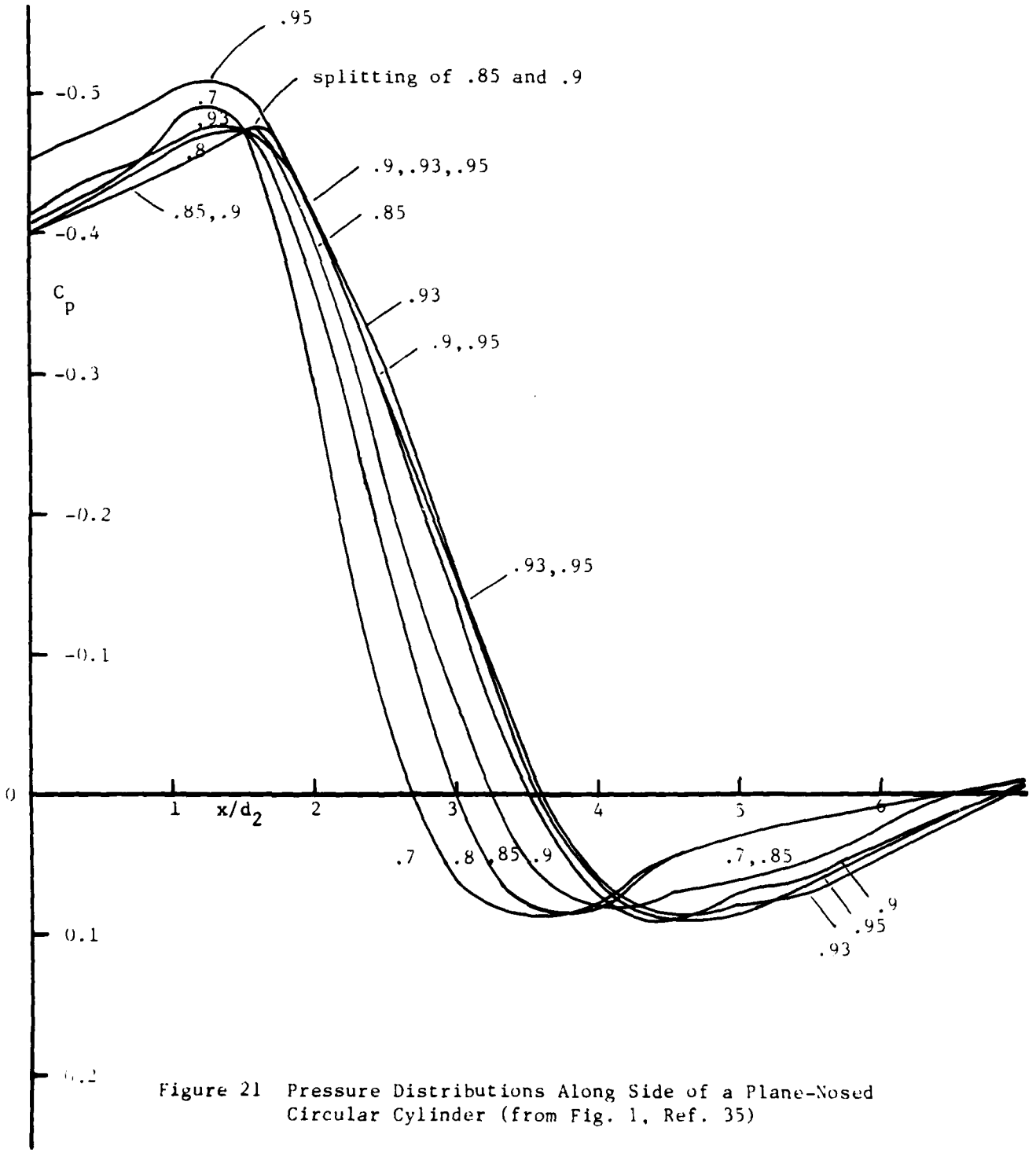

Figure 21 Pressure Distributions Along Side of a Plane-Nosed Circular Cylinder (from Fig. 1, Ref. 35)

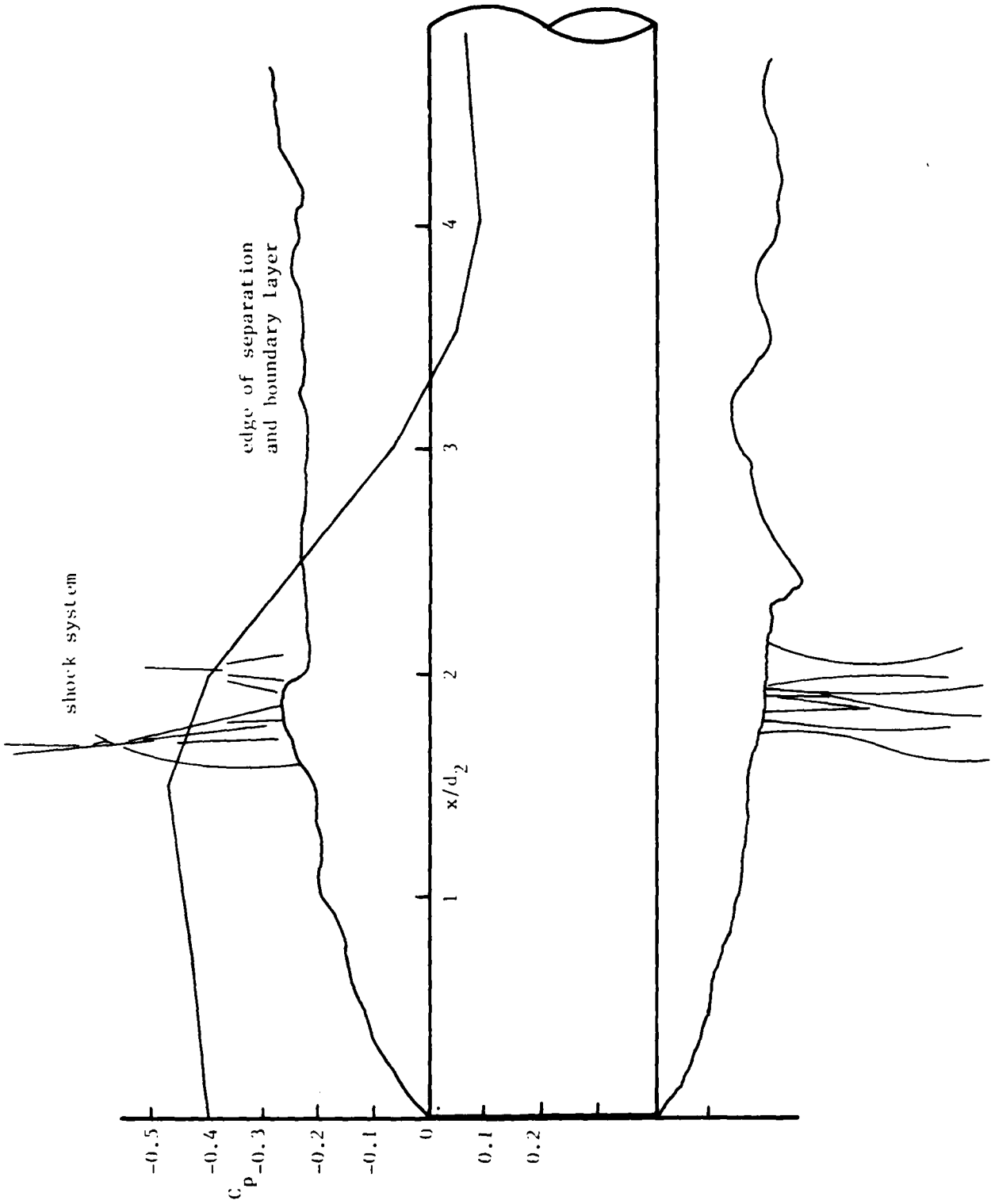

Figure 22a Superposition of Flow Visualization (from Ref. 33) and Pressure Distribution (from Ref. 35) for Plane-Nosed Circular Cylinder at $M_\infty = 0.86$

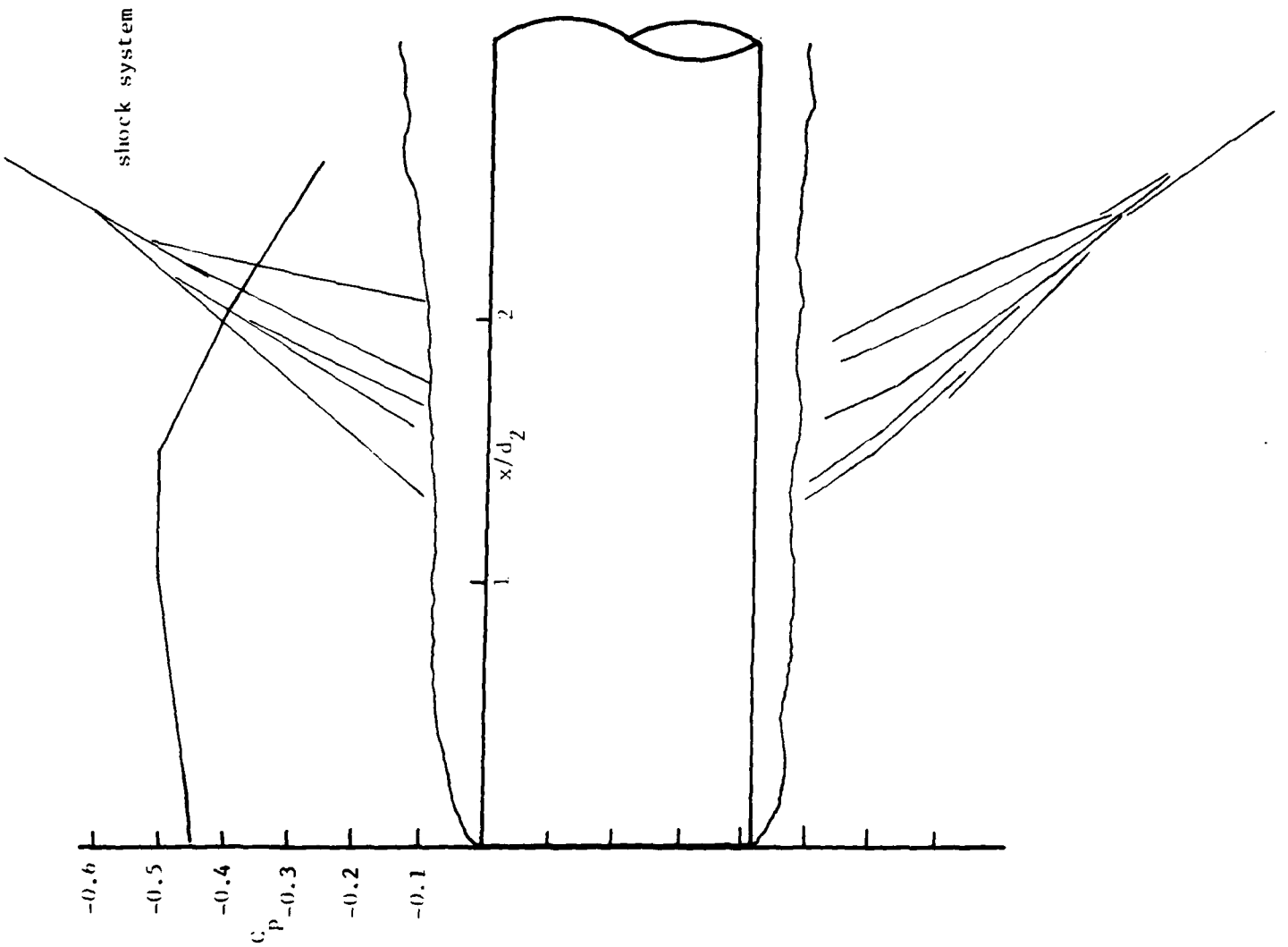

Figure 22b Superposition of Flow Visualization (from Ref. 33) and Pressure Distribution (from Ref. 35) for Plane-Nosed Cylinder at $M_\infty = 1.0$

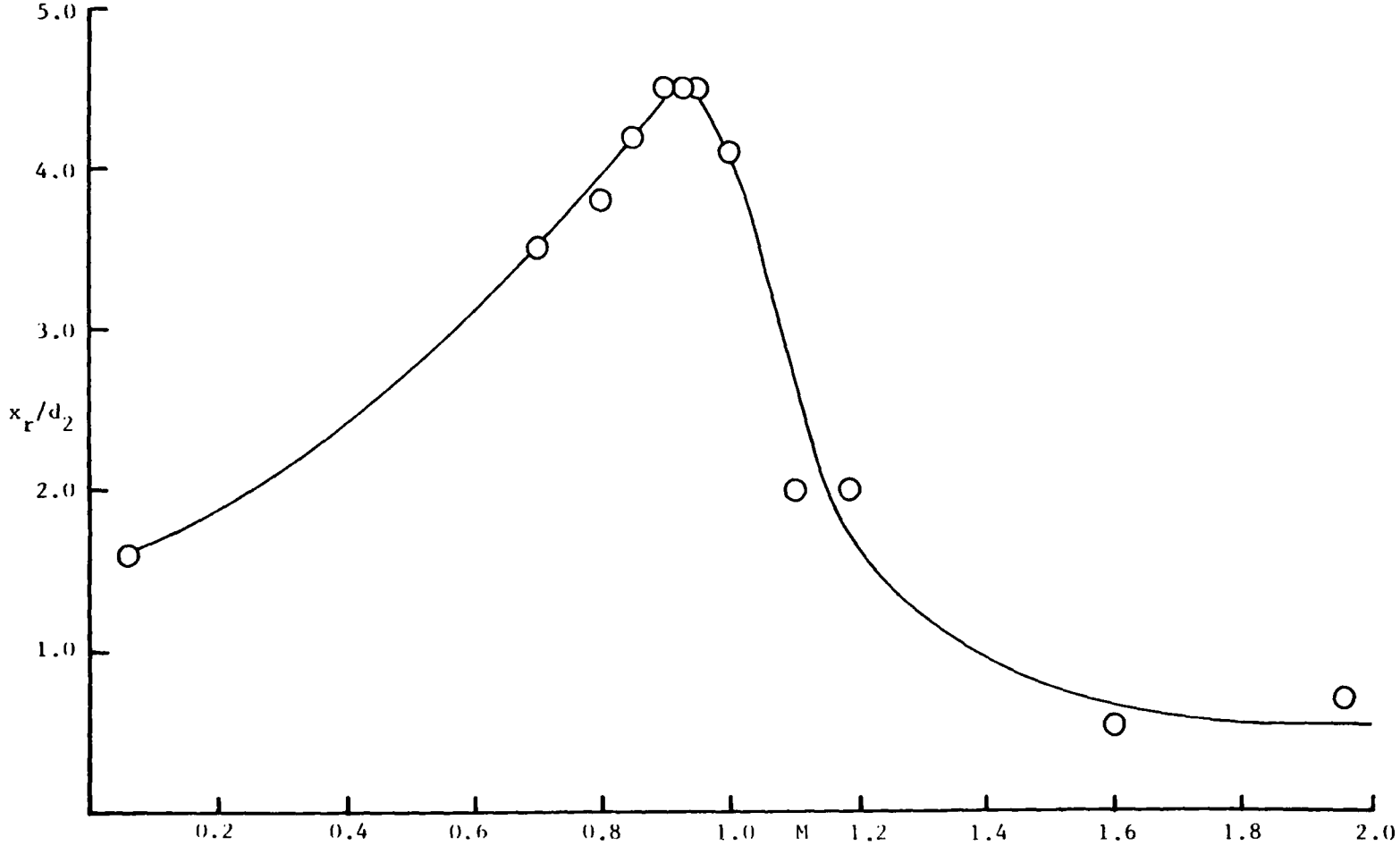

Figure 23 Distance to Reattachment for the Separation from a Plane-Nosed Cylinder (from Ref. 8, 11, 12 and 35)

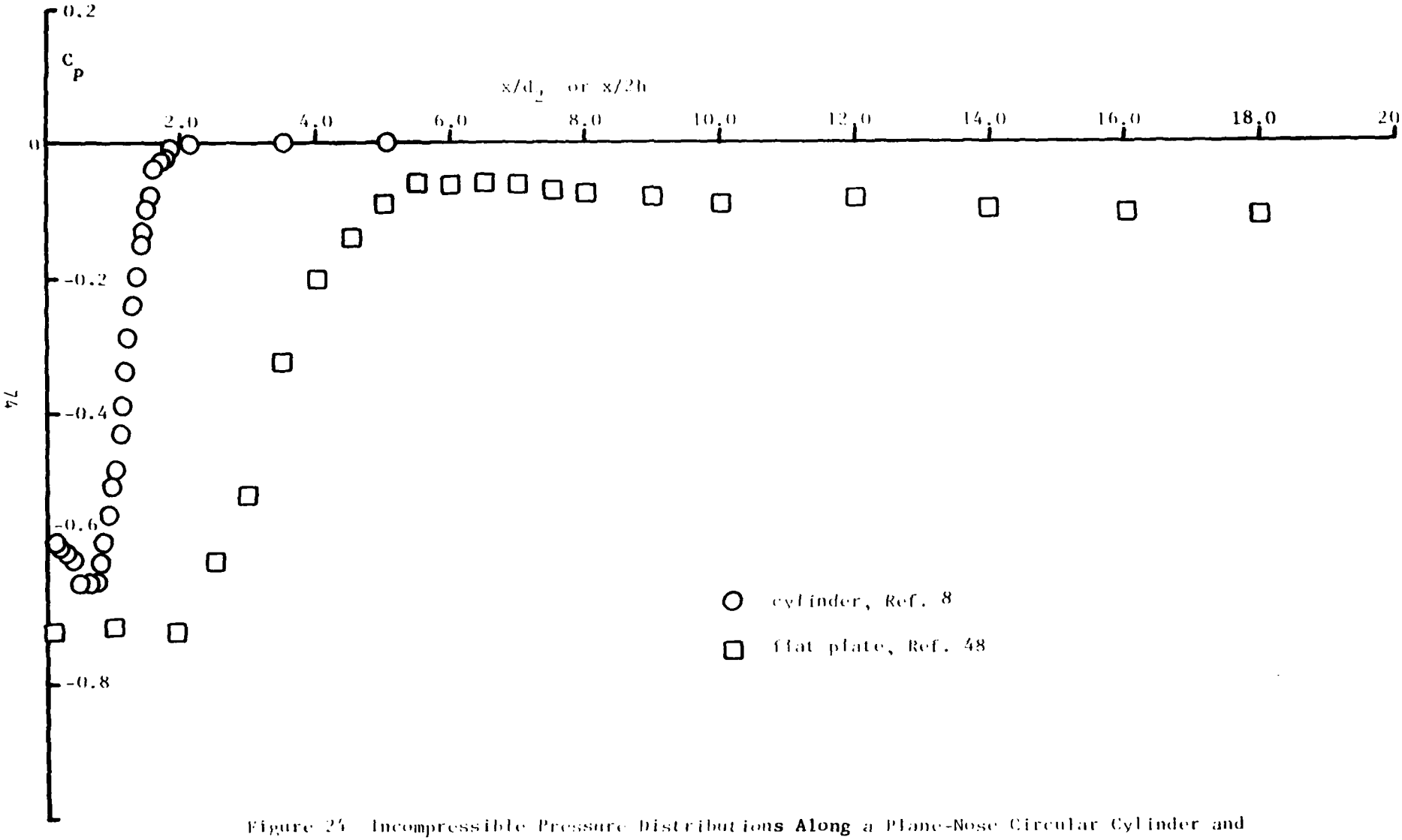

Figure 24 Incompressible Pressure Distributions Along a Plane-Nose Circular Cylinder and Flat Plate (from Ref. 8 and 48)

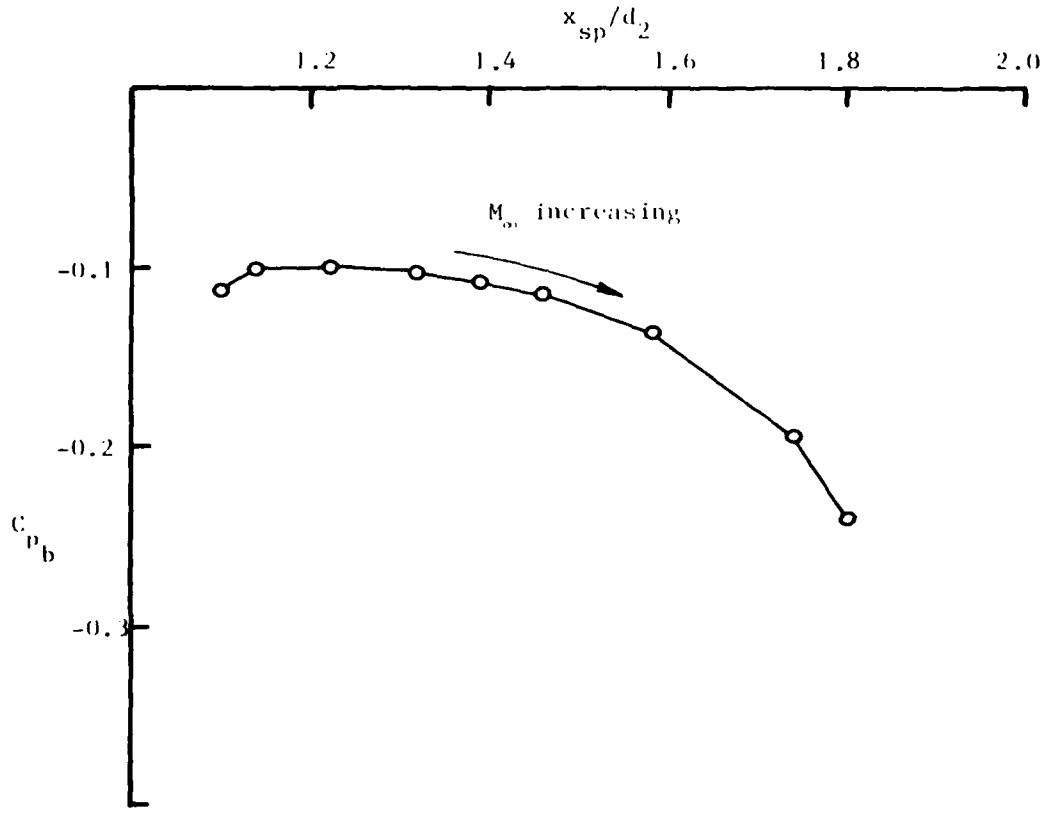

Figure 25 Base Pressure Coefficient and Wake Closure Distance for Blunt-Based Circular Cylinders in Compressible Flow (from Ref. 41)

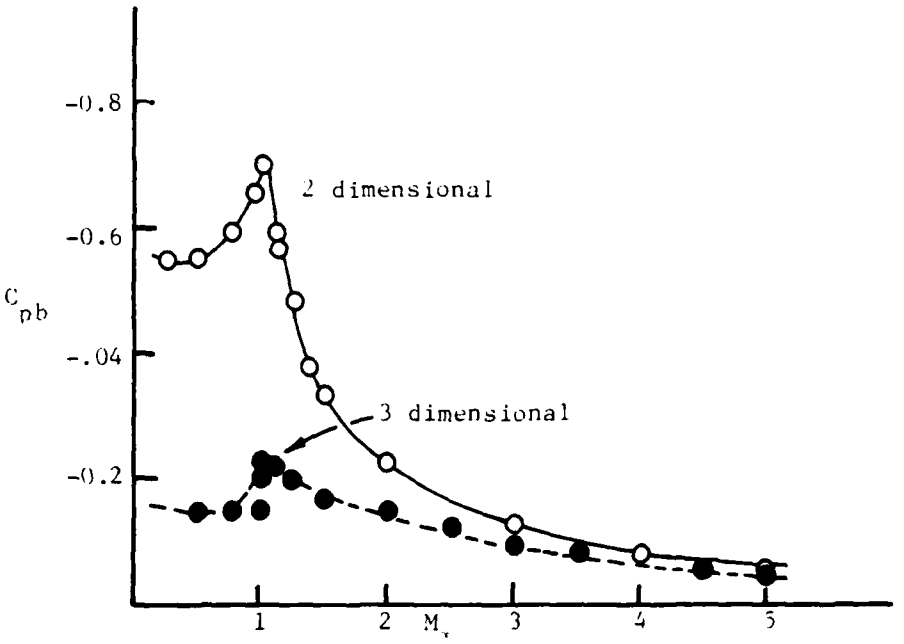

Figure 26 Effect of Geometry on Base Pressure of Blunt-Based Bodies (from Fig. 2.16, Ref. 49)

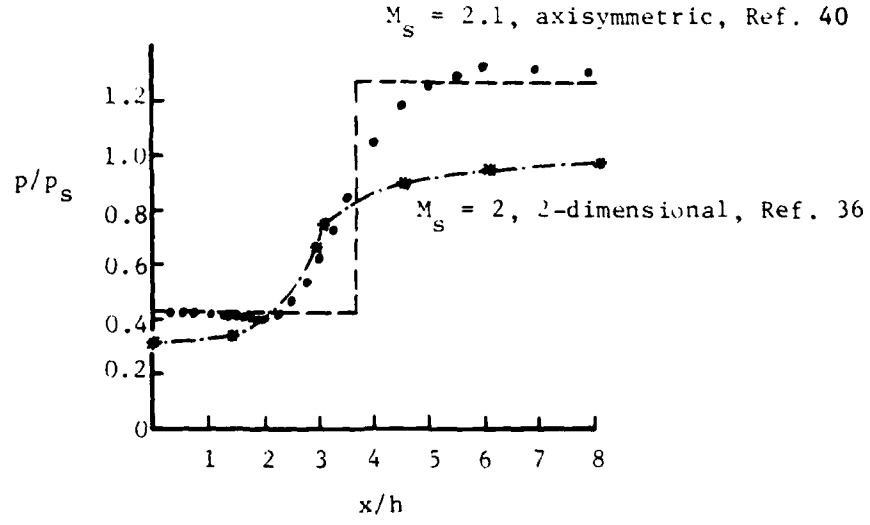

Figure 27 **Effect** of Geometry on the Pressure Distributions for **Downstream**-Facing Steps (from Ref. 36 and 40)

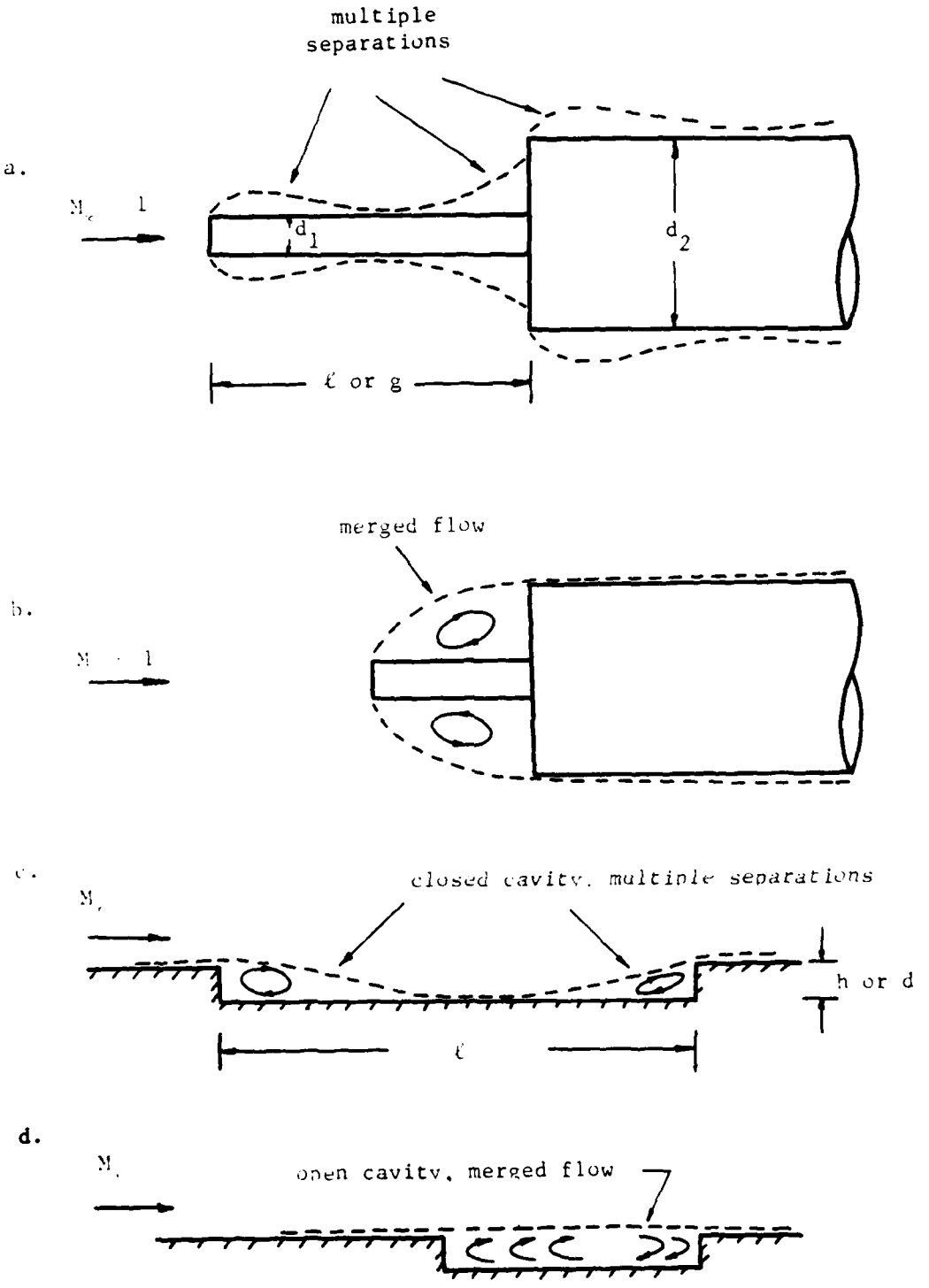

Figure 28 Possible Probe/Cylinder Flows with Analogous Cavity Flows

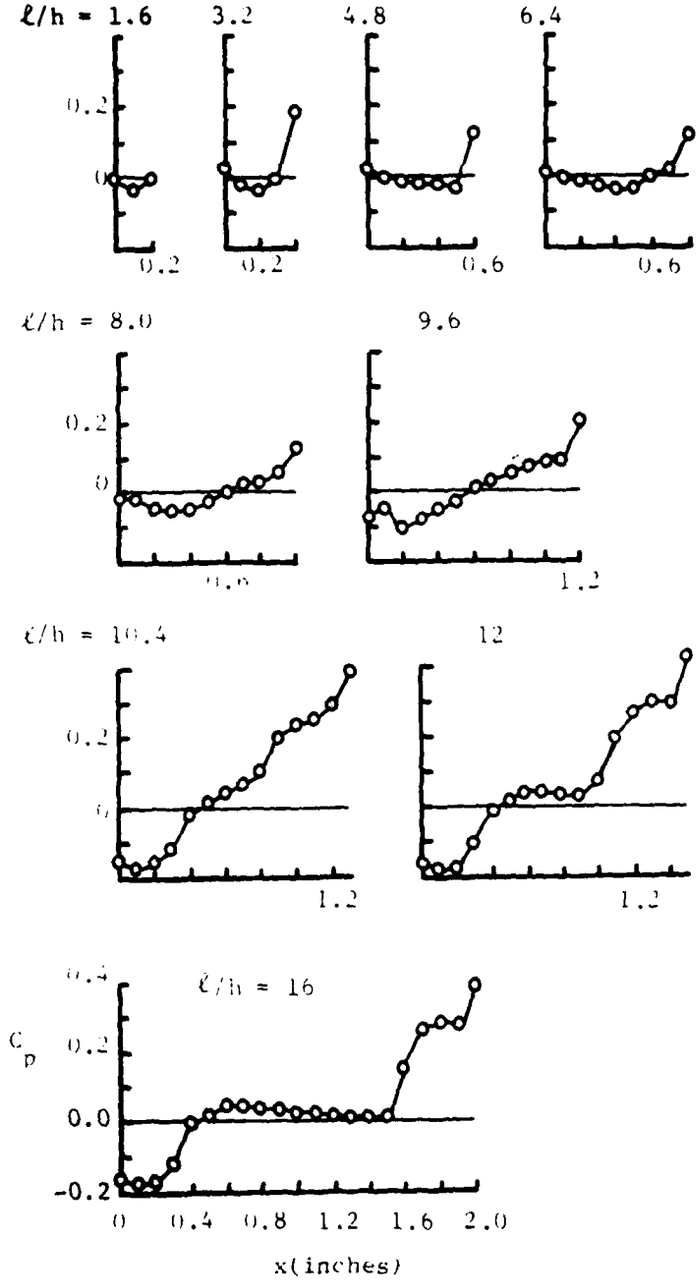

Figure 29 Pressure Distributions Along Floor of an Axisymmetric Cavity for M_∞ = 1.963, h = 0.125 inches, (from Fig. 16, Ref. 39)

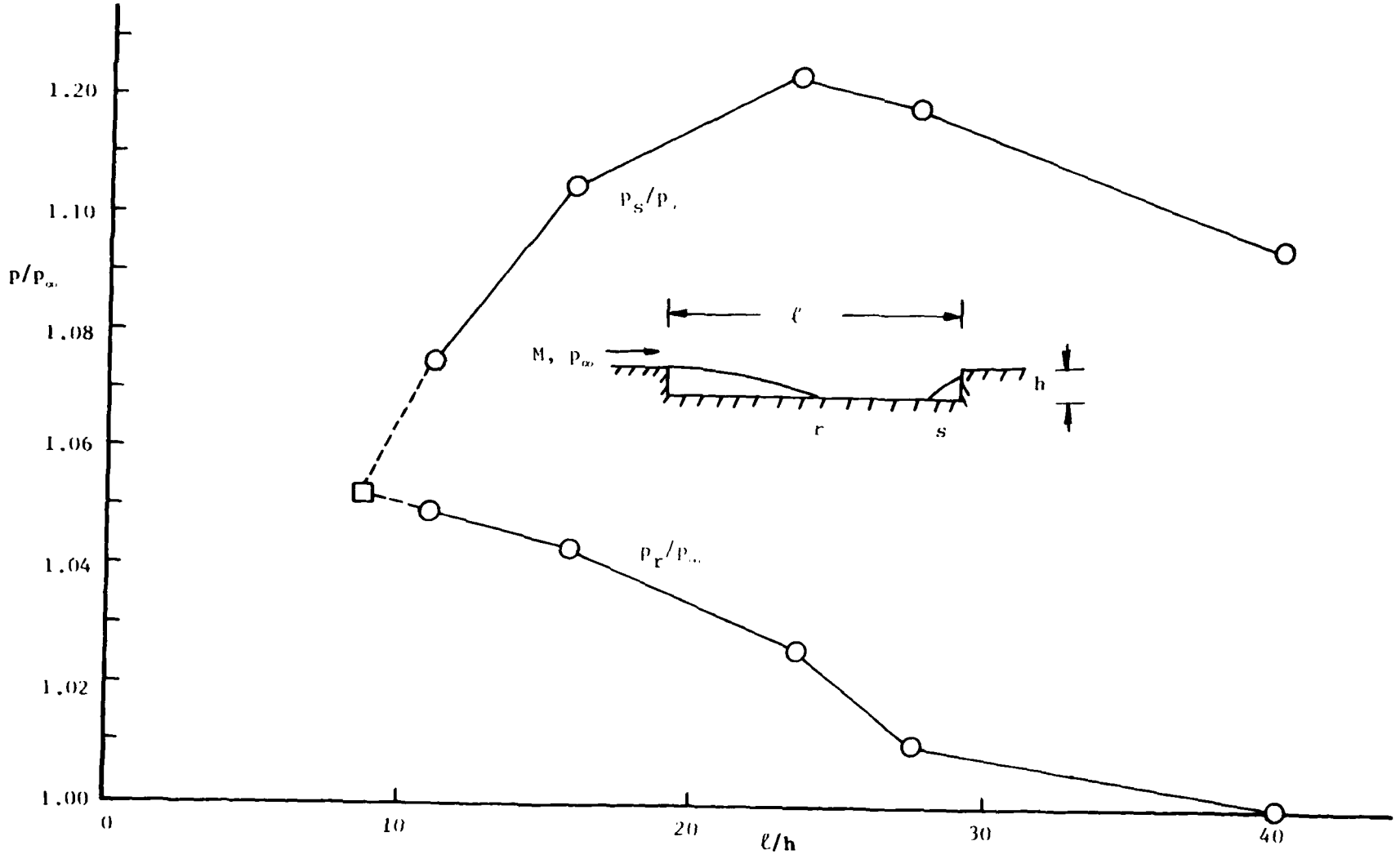

Figure 30 Pressures at Reattachment and Separation for a Closed Two-Dimensional Cavity, $M_\infty = 0.6$ (from Ref. 37)

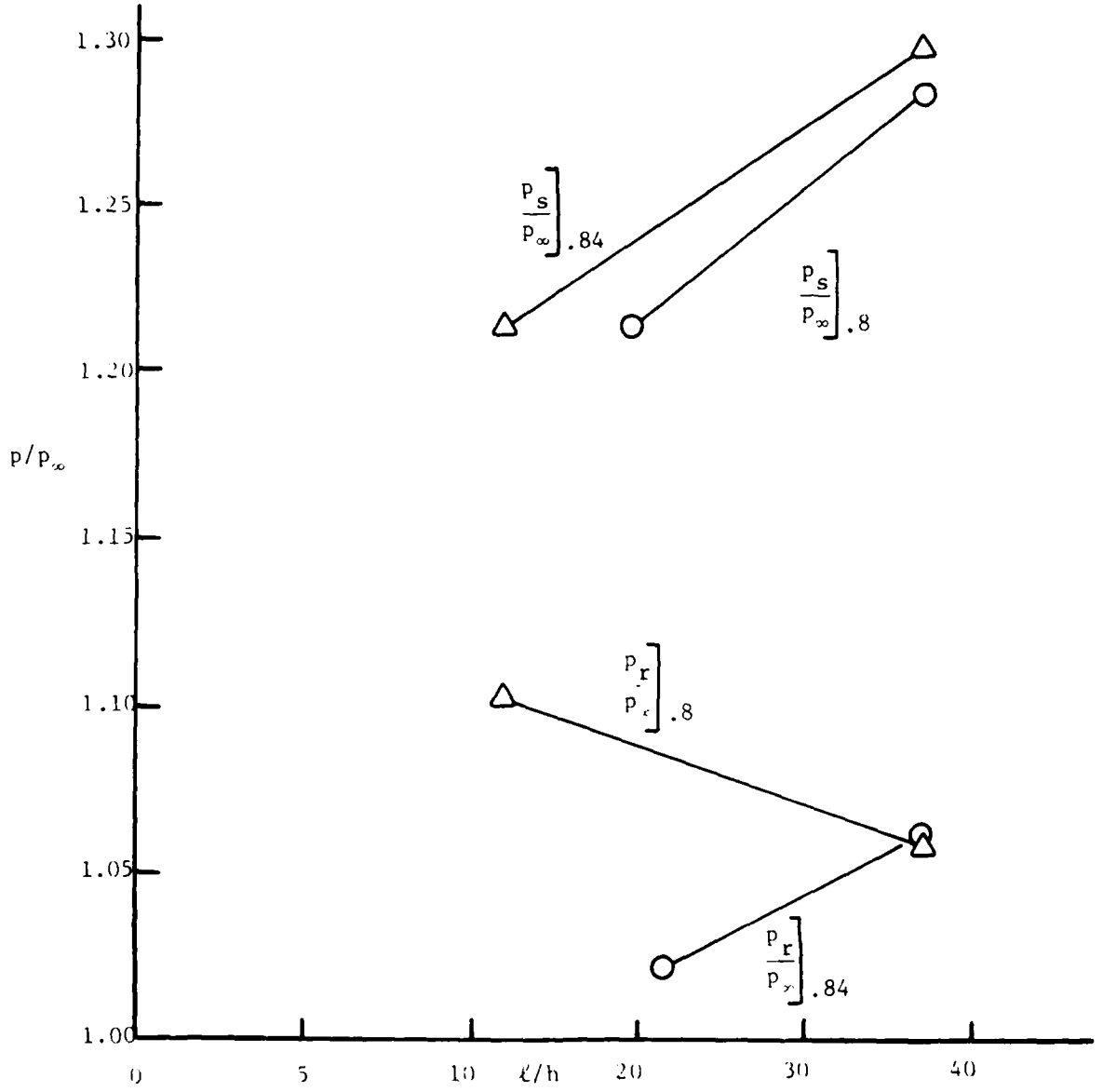

Figure 31 Pressures at Reattachment and Separation for a Closed Two-Dimensional Cavity, M_∞ = 0.8 and 0.84 (from Ref. 37)

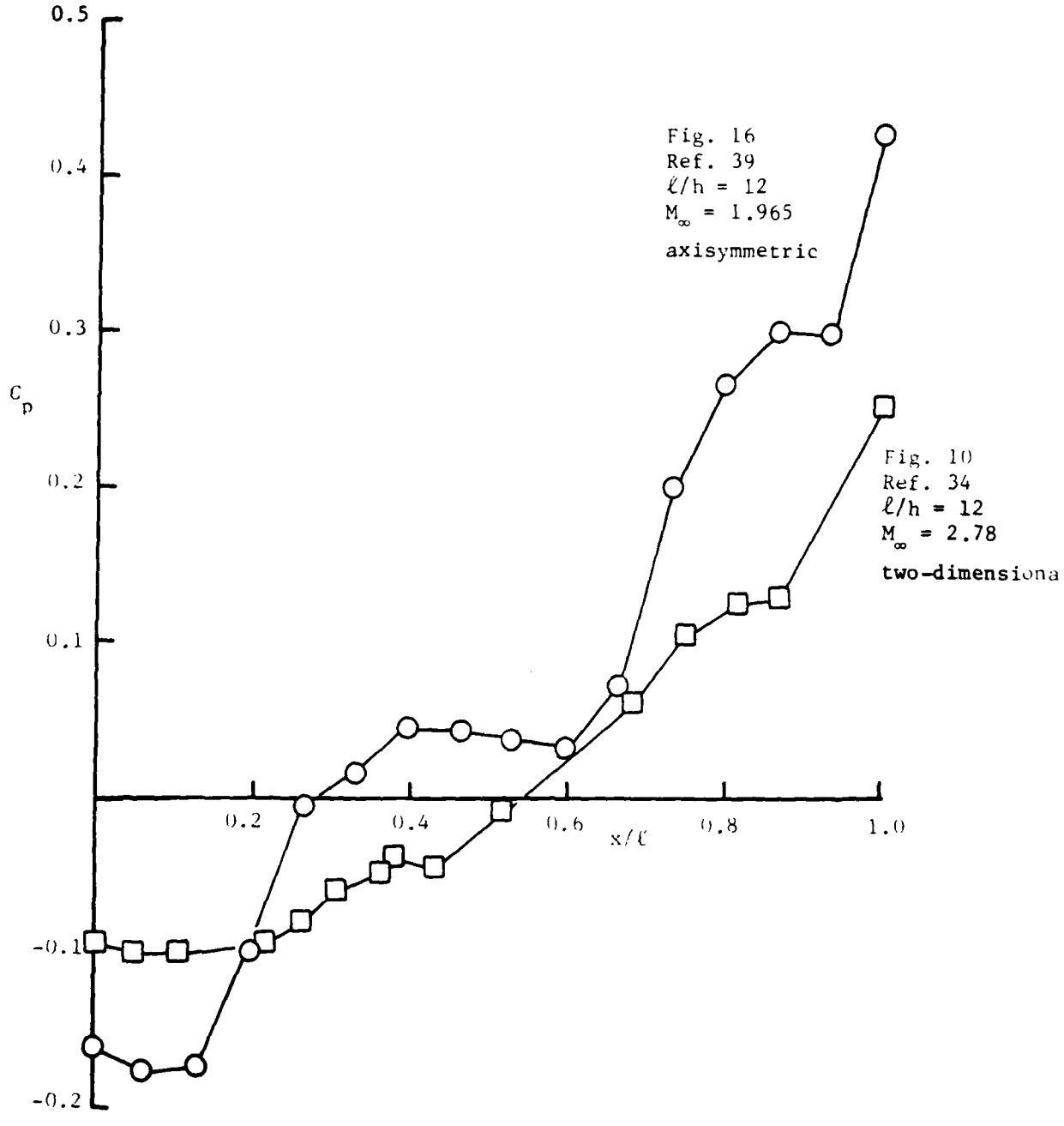

Figure 32 Effect of Geometry on Supersonic Flow Past Cavities (from Ref. 34 and 39)

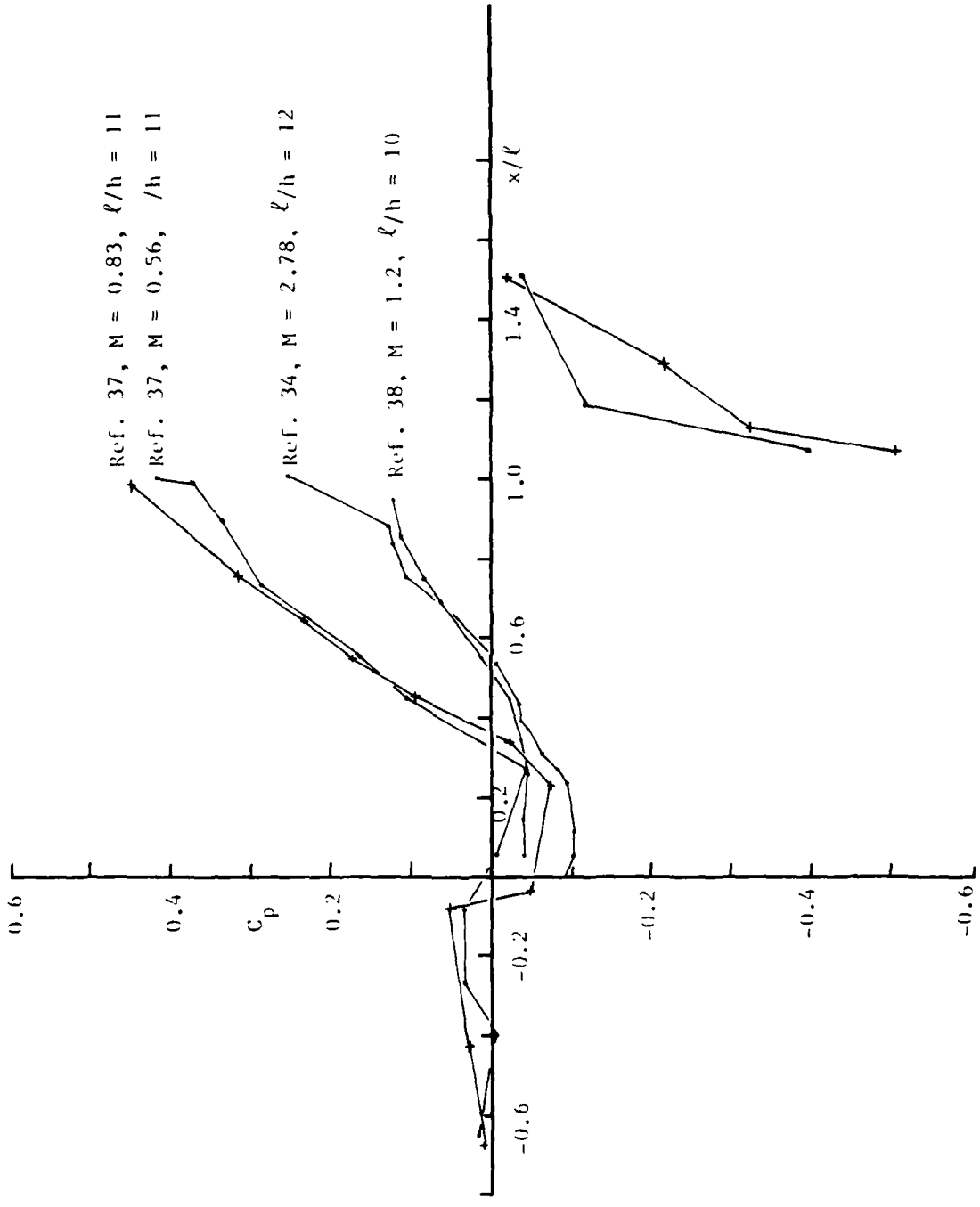

Figure 33 Effect of Mach Number on Flow Past Two-Dimensional Cavities (from Ref. 34, 37, and 38)

AD-A150 667 TRANSONIC MERGING SEPARATED FLOWS(U) MISSISSIPPI STATE UNIV MISSISSIPPI STATE DEPT OF AEROPHYSICS AND AEROSPACE ENGINEERING K KOENIG JUL 84 AFOSR-TR-85-0096 2/2

UNCLASSIFIED AFOSR-83-0179 F/G 20/4 NL

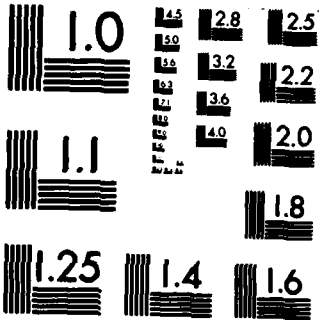

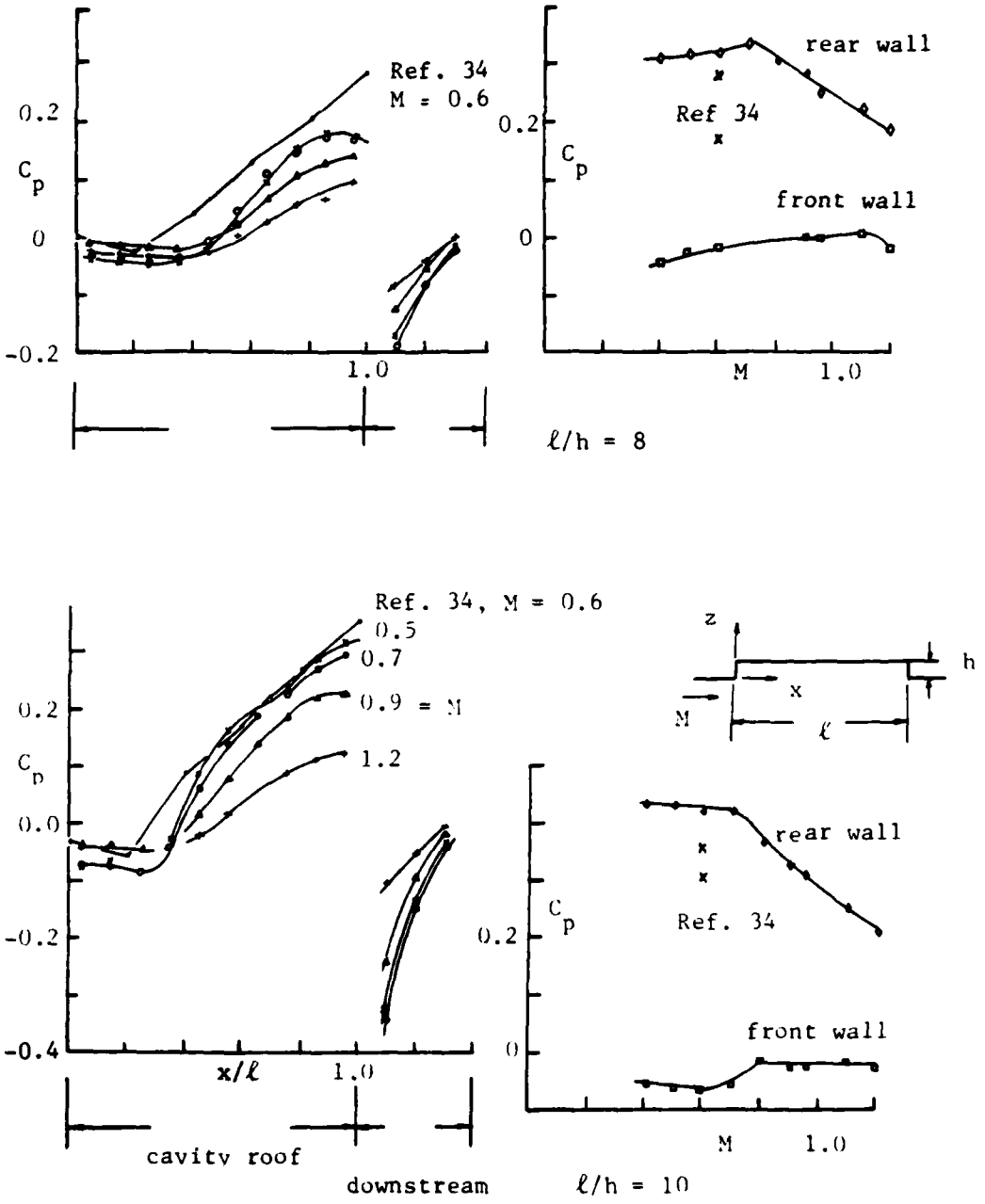

Figure 34 Effect of Mach Number on Flow Past Rectangular Cavities (from Fig. 5, Ref. 38 and Ref. 34)

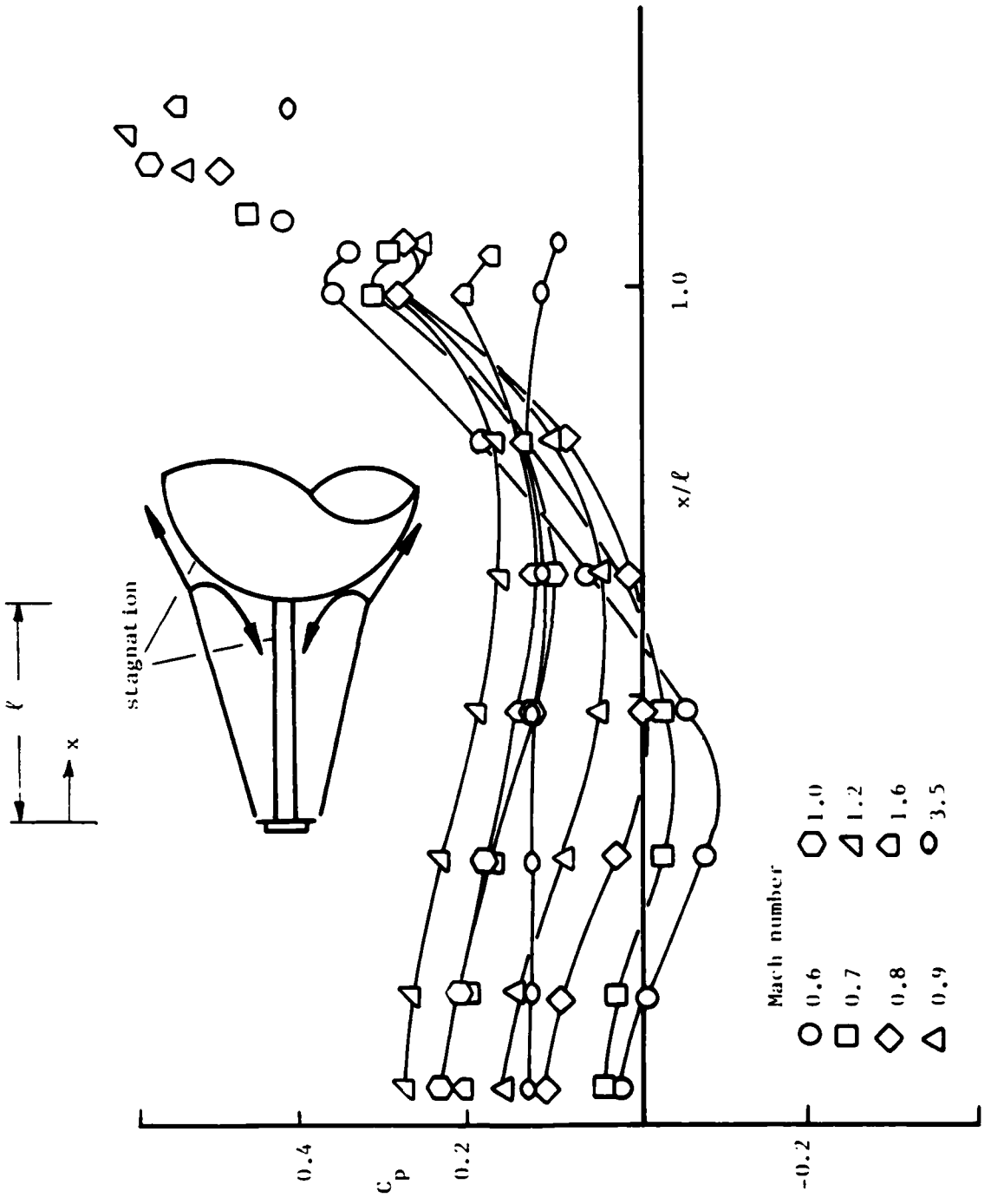

Figure 35 Effect of Mach Number on Flow Past a Spike/Cylinder (from Fig. 5, Ref. 15)

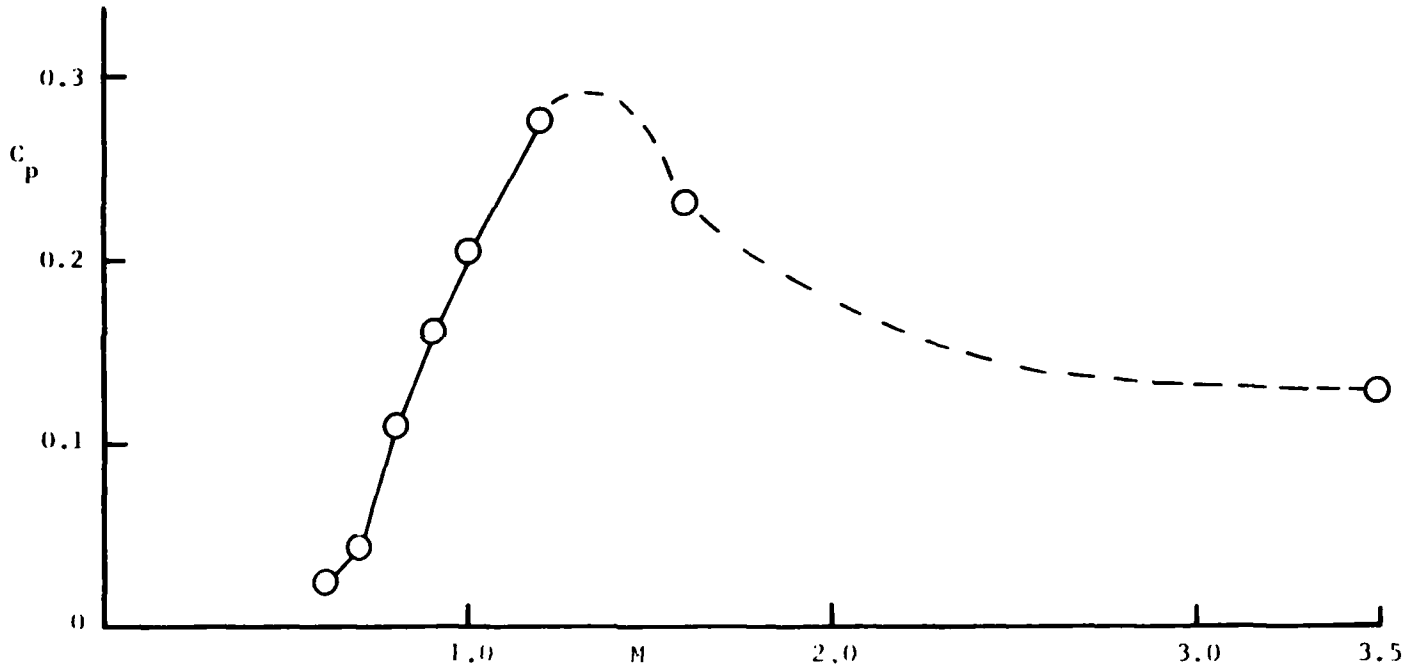

Figure 36 Effect of Mach Number on Initial Separation Pressure for a Spike/Cylinder (from Ref. 15)

END

FILMED

4-85

DTIC